

Review

# Microsystem Advances through Integration with Artificial Intelligence

Hsieh-Fu Tsai <sup>1,2,3,\*</sup>, Soumyajit Podder <sup>1</sup> and Pin-Yuan Chen <sup>1,2,\*</sup><sup>1</sup> Department of Biomedical Engineering, Chang Gung University, Taoyuan City 333, Taiwan; d1131005@cgu.edu.tw<sup>2</sup> Department of Neurosurgery, Chang Gung Memorial Hospital, Keelung, Keelung City 204, Taiwan<sup>3</sup> Center for Biomedical Engineering, Chang Gung University, Taoyuan City 333, Taiwan\* Correspondence: hftsaicgu.edu.tw (H.-FT); pinyuanc@gmail.com (P.-Y.C.);  
Tel.: +886-3-2118800 (ext. 3079) (H.-FT)

**Abstract:** Microfluidics is a rapidly growing discipline that involves studying and manipulating fluids at reduced length scale and volume, typically on the scale of micro- or nanoliters. Under the reduced length scale and larger surface-to-volume ratio, advantages of low reagent consumption, faster reaction kinetics, and more compact systems are evident in microfluidics. However, miniaturization of microfluidic chips and systems introduces challenges of stricter tolerances in designing and controlling them for interdisciplinary applications. Recent advances in artificial intelligence (AI) have brought innovation to microfluidics from design, simulation, automation, and optimization to bioanalysis and data analytics. In microfluidics, the Navier–Stokes equations, which are partial differential equations describing viscous fluid motion that in complete form are known to not have a general analytical solution, can be simplified and have fair performance through numerical approximation due to low inertia and laminar flow. Approximation using neural networks trained by rules of physical knowledge introduces a new possibility to predict the physicochemical nature. The combination of microfluidics and automation can produce large amounts of data, where features and patterns that are difficult to discern by a human can be extracted by machine learning. Therefore, integration with AI introduces the potential to revolutionize the microfluidic workflow by enabling the precision control and automation of data analysis. Deployment of smart microfluidics may be tremendously beneficial in various applications in the future, including high-throughput drug discovery, rapid point-of-care-testing (POCT), and personalized medicine. In this review, we summarize key microfluidic advances integrated with AI and discuss the outlook and possibilities of combining AI and microfluidics.



Citation: Tsai, H.-F.; Podder, S.; Chen, P.-Y. Microsystem Advances through Integration with Artificial Intelligence. *Micromachines* **2023**, *14*, 826. <https://doi.org/10.3390/mi14040826>

Academic Editors: Nam-Trung Nguyen and Daniel Ahmed

Received: 9 March 2023

Revised: 4 April 2023

Accepted: 6 April 2023

Published: 8 April 2023



**Copyright:** © 2023 by the authors. Licensee MDPI, Basel, Switzerland. This article is an open access article distributed under the terms and conditions of the Creative Commons Attribution (CC BY) license (<https://creativecommons.org/licenses/by/4.0/>).

## 1. Introduction

The study and control of fluids in channels and systems with perimeters generally between a few micrometers to a few millimeters is known as microfluidics [1]. The microfluidic flows are typically of low Reynolds number, i.e., viscous forces outweigh inertial forces, and are thus laminar in nature [2]. The high surface-area-to-volume ratio in microfluidics enables faster heat and mass transport, which enhances reaction control and speeds up reaction time [3]. The microfluidics discipline entails the theoretical and technological development of accurate manipulation of microscopic fluid volume and examination of phenomena occurring within it. Applications using microfluidic devices can be found in broad domains across biomedicine, chemistry, and material science [4–6].

A branch of artificial intelligence called machine learning is concerned with creating algorithms that can learn from data and establish the association between data and the

features of interest [7]. Moreover, the iterative update of parameters in machine learning algorithms allows their accuracies to increase when the algorithms “learn” from additional data. Furthermore, development of artificial neural networks (ANNs) has advanced artificial intelligence in recent decades, particularly in image and language recognition [8,9]. In neural networks, influenced by applied mathematics, physics, and neuroscience, artificial neurons are mathematically modeled and arranged in layers to process information similar to how biological neurons would be. During training, the weight of each association between neurons is updated by backward propagation to establish the association between data and features [10]. In deep learning, as the neural network layers deepen and the number of neurons increases, more data are required, but patterns in complex data can be recognized [11]. As a result, the training of it becomes more computationally demanding, but through the advances of parallel processing offered in the graphics processing unit (GPU), the field of deep learning continues to thrive and has seen innovation to various applications such as self-driving car, security, drug development, and medical image diagnosis [12–17].

Intelligent microfluidics, a field enabled by the integrating the data processing capability of machine learning and data science with the automation potential in microfluidics [18], is particularly effective in advancing quantitative biology and rapid medical diagnostics [19]. Next-generation biomimetic microfluidic systems such as organ-on-chips (OoCs) have great potential to recapitulate and model human physiological as well as pathophysiological processes *in vitro*. The complex and vast amounts of high-throughput data generated on these platforms are also great opportunities for AI.

In this review, we discuss the development, applications, and outlook of intelligent microfluidics, where advancements are made through integration between microfluidics and artificial intelligence (Figure 1).

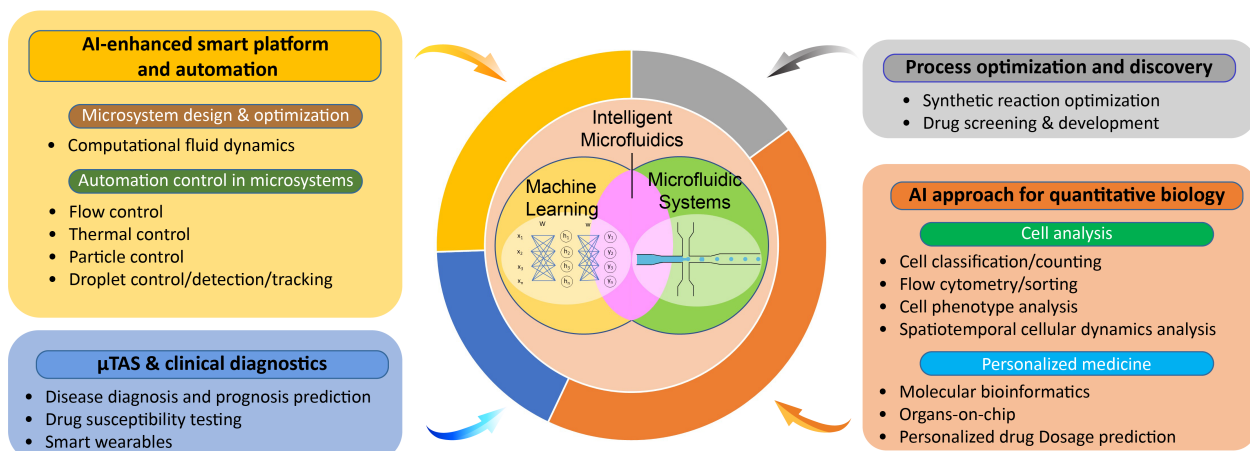


**Figure 1.** Diagram of microfluidic applications integrated with artificial intelligence (AI). μTAS stands for micro-total analysis systems.

## 2. AI-Enhanced Smart Platform and Automation

### 2.1. Computer-Aided Microsystem Design and Optimization

Microfluidic chips take advantage of physical phenomena at smaller length scales; therefore, miniaturization of these devices often requires customized design. Recent advances in machine learning have been applied to the design and optimization of microfluidic systems [20].

The entire hydraulic circuit and components within it can be analyzed and optimized using circuit modeling [21–25]. Several machine learning and numerical simulation methods have been applied to microdevice design for flow sculpturing [26–28], micromixing [29–32], microjetting [33], droplet microfluidics [34,35], and extensional rheometry [36]. For example, a convolutional neural network (CNN) is trained to learn the

sculpturing outcome of flow due to micropost locations in the microfluidic channel; the system has improved performance over conventional computational fluid dynamics (CFD)-based forward models and can potentially predict results when the condition is outside the scope of what was used in the training (Figure 2a) [27]. By taking the AI approach, design iteration of microfluidic chip can be rapidly accelerated.

Moreover, machine learning techniques can also be applied to the fabrication of Microsystems. For example, Wang et al. adapted a fully automated CNN computer vision system to aid in calibration during 3D printing of microstructure dimensions [37]. Shchanikov et al. used an ANN to design a bidirectional biointerface with nanoelectronics and microfluidics [38]. Contemporary numerical simulation software can readily integrate with machine learning techniques to iterate microdevice designs, accelerating device development and validation, e.g., the ones used for particle trajectory prediction can be adapted for predicting red blood cell (RBC) movements in microchannels [39–41].

### Computational Fluid Dynamics (CFD) Modeling

In recent years, advances in GPUs have made the training of deep ANNs possible. The features in structured data sequences, images, and videos can be quickly learned and inferred in modeling fluid dynamics [42–44].

In continuous-flow microfluidics, Cai et al. introduced artificial intelligence velocimetry (AIV), which integrated imaging data with physics-informed neural networks, to measure the velocity and stress fields of blood flow [45]. By utilizing neural networks to automatically evaluate experimental data and infer important hemodynamic markers that quantify vascular damage, AIV offered a novel paradigm that seamlessly blended pictures, experimental data, and underlying physics. Similarly, the flow velocity profile in a shallow microfluidic channel could also be extracted from the scalar signal transport through a deep neural network [46]. In microfluidic systems, often a system is in the laminar regime with low Reynolds number and high Péclet number, which means that viscous force and advection are more dominant than effects from inertia and diffusion. In certain applications, such as concentration gradient generation and chemical synthesis, mixing efficiency in microchannels becomes important. The fluid behavior in microstructure-based passive microfluidic mixers can be predicted using AI, and designs can be rapidly iterated in comparison to conventional physics-coupled numerical simulations where flow field and chemical transport has to be sequentially solved [29–32,47].

Multiphase flow is also a discipline that has many applications, such as two-phase emulsion, protein extraction in biotechnology, and injection molding in manufacturing. The flow pattern in two-phase fluid mixing can be rapidly modeled using neural networks trained with physical knowledge and comparable to that by classical CFD solutions, where approximation to Navier–Stokes equations requires large amount of computational resources [48–51]. Moreover, combinatorial multiphase flow can be utilized to assemble colloidal materials in microfluidics, and machine learning can accelerate the predictability of material characteristics for designing such materials [52]. An AI algorithm to predict multiphase fluid dynamics can accelerate and aid in the design of microfluidic chips for these applications.

## 2.2. Automation Control in Microsystems

### 2.2.1. Flow Control

The flow in microfluidics can be actuated by pumps of different mechanisms, such as syringe-driven, peristaltic, pressure-driven, piezoelectric, electro-osmotic, or microvalve-based peristaltic micropumps [53]. Dynamic laminar flow control by pistons or syringe pumps is required in applications where joining flow boundary location requires precise control and syncing. Dressler et al. developed a reinforcement learning-based deep Q network that utilized image feedback for rapid and high accuracy flow control and droplet size control [54].

Micropumps composed of microvalves or piezoelectric valves often become important components due to their ability to integrate into the microdevice and to realize the development of the micro-total analysis system ( $\mu$ TAS) [55]. Abe et al. used reinforcement learning for timing control of valve operation in peristaltic micropumps to increase the maximum flow rate [56,57]. Integration of multiple microvalves into a fully programmable biochip was designed by Shayan et al. [58]. Integration of machine learning techniques with the fully programmable platform enables real-time detection of biochip status and detection of potential attacks against a real-world bioassay.

## 2.2.2. Thermal Control

The advances in microelectromechanical systems (MEMS) continue to decrease the size and increase the power, therefore thermal management on MEMS devices becomes a vital component to the system. Due to the small length scale and small thermal resistances in microfluidics, a microfluidic heat sink was applied for cooling MEMS chips [59]. Moreover, precise heating or cooling of microfluidics is also important for applications in  $\mu$ TAS [60].

High speed and accurate thermal control of a microfluidic platform is made possible by the use of an ANN trained on infrared (IR) thermography [61]. Quinn et al. also reported an optically controlled thermofluidics platform with machine learning feedback control [62].

As an alternative to passive thermal measurement using IR thermography, temperature-sensitive species can be introduced to the system and report local temperatures in the microenvironment, such as nanocrystals or quantum dots. However, the temperature often needs to be inferred from photoluminescence data and the accuracy is poor. By applying a fully-connected ANN, Lewis et al. demonstrated that improved accuracy and temporal resolution of temperature in the local microenvironment were obtained using cadmium telluride (CdTe) quantum dots [63].

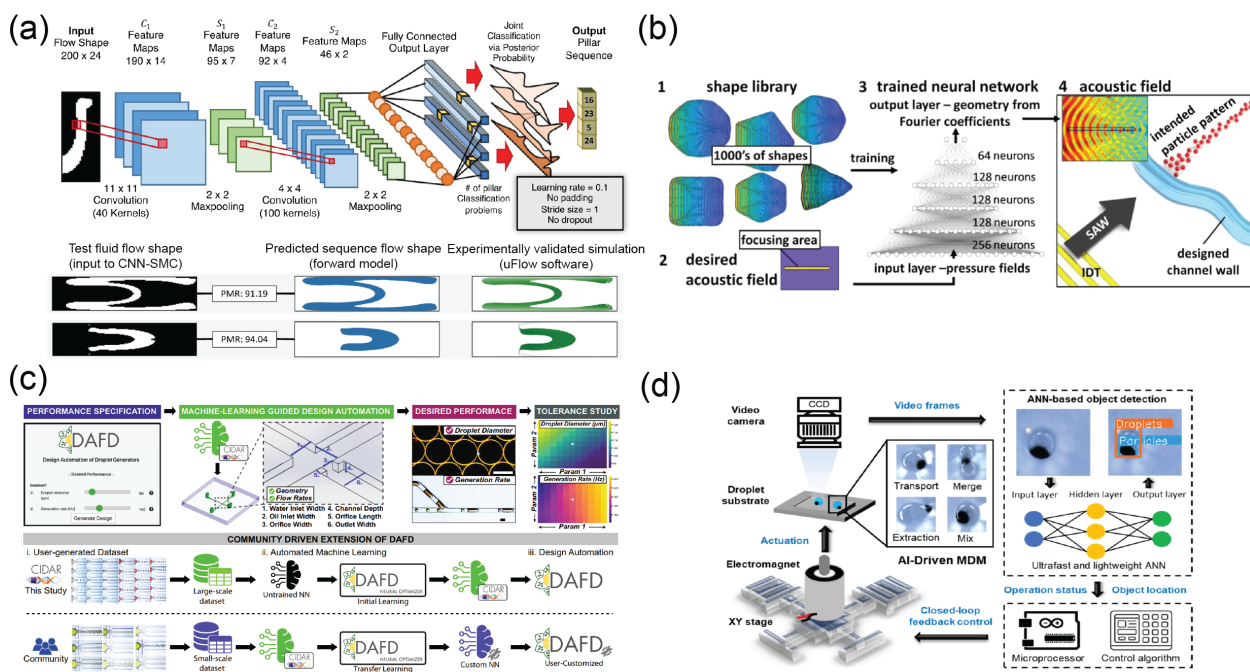


**Figure 2.** Selected examples of AI-enhanced smart platforms and automation. **(a)** A CNN framework to predict the outcome of flow sculpturing by micropillar microstructures [27]. Reproduced under Creative Commons Attribution 4.0 International license (CC-BY). **(b)** A DNN to predict particle patterning by surface acoustic waves in a shape library was proposed by Raymond et al. [64]. Reproduced under CC-BY license. **(c)** Machine-learning-empowered design automation of droplet microfluidics channel [34]. Reproduced under CC-BY license. **(d)** Machine-learning-assisted classification for droplet manipulation in a magnetic digital microfluidic platform [65]. Reproduced under CC-BY license.

### 2.2.3. Particle Manipulation

In many applications, such as separation, diagnostics, and patterning, particle manipulation is often a required process. The low reagent requirements and smaller length scale make microfluidics a good candidate platform for such applications [66]. The particle manipulation can be exerted through electromagnetic, optical, hydrodynamic, or acoustofluidic techniques, while machine learning methods can be further adapted for precise and rapid control.

The particles in the fluid system can be manipulated through flow dynamics. Fang et al. used an ANN-based feedback pump control to create a hydrodynamic Stokes trap for particle manipulation [67]. Through reinforcement Q-learning, Abe et al. also demonstrated that a micropump-based system can learn to control and manipulate a microparticle to reside in a predefined target area [57]. Particles in a curved channel or in a straight channel filled with viscoelastic fluids also experienced inertial motion and were manipulated [68,69]. Recently, Su et al. and Hamdi et al. separately reported AI-accelerated approaches to calculate lift coefficient in microfluidic channels for inertial focusing based on knowledge from the computationally-expensive direct numerical simulation method [70,71].

Magnetic particles can also be conjugated to a desired biorecognition element, and an external magnetic field can be applied for magnetophoretic isolation [72]. Koh et al. combined magnetophoresis with supervised learning for sorting and purification of normal sperm based on the slender body theory [73]. Optical power of light can also exert forces on microscopic particles in the optical tweezers technique. While conventional control theory such as the proportional–integral–derivative controller is commonly adapted, machine learning techniques can also be used to increase speed and accuracy when calculating the optical force and manipulation [74,75].

In the field of acoustofluidics, where a piezoelectric actuator or platform is used, the particles can be spatially manipulated based on their acoustophysical properties, typically through a feedback control [76]. Raymond et al. trained a DNN on pictures of presolved acoustic fields to allow rapidly tailored acoustic fields for patterning microparticles in microchannel components (Figure 2b) [64]. By using AI to predict the acoustic field, the design of an acoustofluidics chip can be optimized and automated for tailoring specific applications. While conventional numerical and analytical solutions are used to resolve acoustic pressure fields in designed geometry, the inverse problem can be resolved more efficiently by taking the DNN approach. Similarly, Yiannacou et al. demonstrated that control of a single ultrasound transducer frequency through an epsilon-greedy algorithm can be used to control and manipulate the particles [77,78].

### 2.2.4. Droplet Control, Detection, and Tracking

Droplet microfluidics is a particular case of multiphase microflow, where two or more immiscible fluids are split into single or multiple emulsions as tiny liquid reactors for bioanalysis, chemical synthesis, cell culture, and more [79,80].

To produce droplets of desired size, precise control and minimization of variation of flow rates are essential [54]. Mahdi and Daoud demonstrated that an ANN can be used to predict the size of microdroplets [81]. Lashkaripour et al. proposed a web-based software tool, DAFD, with machine learning algorithms to predict droplet formation performance with a high level of accuracy in a flow-focusing microfluidic chip (Figure 2c) [34]. The machine learning algorithm can also automate the microfluidic chip design for a specific droplet size desired by the user. In particular, the DAFD software was designed for scientific community collaboration, where the machine learning algorithms can learn both from the data in the developer's laboratory and from volunteered data from the community. The federated learning approach can aid in creating a universal neural network for data collected in different settings [82]. Similarly, Siemenn et al. adapted a Bayesian inference with droplet size measurement feedback from images to optimize droplet generation [83]. The stability of microdroplets can be significantly affected by the type of surfactant and its concentration. Khor et al. established a convolutional autoencoder model to anticipate

if a droplet would become unstable and break up [84]. Chagot et al. utilized a Bayesian regularized ANN and XGBoost algorithms to predict droplet size given flow rate and surfactant concentrations with mean absolute percentage error as low as 3.9%, in comparison to other state-of-the-art models [85].

Droplet segmentation and classification in images can be achieved using machine learning techniques as well. Various versions of CNN-based You Only Look Once (YOLO) object detectors have been used for automated detection of droplets and content within them at frame rates of up to 100 frames per second (FPS) [86,87]. Subsequent tracking of droplets to extract droplet dynamics is also practiced using deep learning techniques under brightfield and fluorescence microscopy [88,89].

In machine learning, the algorithm learns to establish the association between features and data. Therefore, a trained neural network can also predict the experimental conditional from image results [90]. For example, the microdroplet images can be predicted by a trained deep neural network for the flow rate or concentration used based on the droplet's size and optical property, reaching accuracy within 0.5% [91]. Arjun et al. also reported that droplets with various chemical mixing efficiencies can be classified by a trained CNN [92]. Droplet freezing and extrapolation of exact temperature for ice nucleation on a microfluidic freezer platform was made possible using a DNN model with a polarized light detection [93]. Tang et al. reported an ANN to classify microdroplets containing magnetic particles and showed its manipulation with failure-correction capability, demonstrating the superiority of ANN compared to conventional magnetic digital microfluidic platform [65] (Figure 2d). The integration of AI-based image analysis in the automation and control process of the digital microfluidic platform provides additional advantages of quality assurance and online decision making.

After detection and classification of desired droplets, fluid routing or sorting can be integrated in the downstream microfluidic component to isolate them. Automated routing of droplets has been demonstrated using deep reinforcement learning [94] and evolutionary algorithms [95]. Alternatively, droplets containing desired products such as cells or particles can be sorted as well when the AI for the detection is combined with an active component for target purification [96–98].

### 3. Process Optimization and Discovery

#### 3.1. Synthetic Reaction Optimization

One advantage of AI is its ability to sequentially generate a large amount of experimental parameters for automated iteration, and it also discerns patterns in the result. Therefore, many applications exist that automate microfluidics with AI for large-scale experimental iteration in medicine, material science, and energy development [18,99].

For chemical synthesis, machine learning algorithms can be used to automate the experiments and optimize based on feedback when combined with robotics [100–102]. McMullen and Jensen demonstrated an automated microreaction system incorporated with silicon-based microfluidic devices and machine learning for optimization of synthesis without the need for *priori* information, i.e., a “black-box” optimization, to the reaction parameters [103,104] (Figure 3a), which means the microreaction system can be placed in continuously self-optimization to find the reaction parameters for best product properties set by the designer. Rizkin et al. used a machine learning algorithm with IR monitoring to automate microchemical reactors in the polymerization of zirconocene [105]. The parameters of the chemical kinetics of a complex reaction can also be modeled with the aid of machine learning, leading to a broad technoeconomic outcome.

#### 3.2. Nanoparticle Synthesis

Control of flow rate, concentration, and mixing are vital variables for nucleation and synthesis of nanoparticles on the microfluidic platform and one of the applications adapting AI [106]. Krishnadasan et al. adapted a noise-tolerant global search algorithm for a black-box optimization of injection rate and temperature for synthesizing CdSe nanoparticles on

a Y-shaped microfluidic reactor from CdO and Se precursor solutions [107]. Similarly, ANN can be used to extract the condition–property relationship from the combinatorial synthesis data and provide conditions to synthesize nanoparticles [108–113], nanotubes [114], nanoformulation of pharmaceuticals [115], quantum dots [116,117], liposomes [118], or polymeric microparticles [119,120] (Figure 3b). Diamanti et al. trained an ANN to predict particle size of poly(Lactide-co-glycolide) (PLGA) microparticles, a biocompatible drug delivery polymer, based on the conditions of the flow focusing synthesis experiments on multiple different synthesis platforms. The learnability or the trainability of the AI enables the *in silico* size-dependent design of microparticle synthesis for tailored applications.

Notably, the trainability of neural networks not only provides an optimization method for synthesis in that early stage when the data size is small but can also continue to refine through learning the new data and further feedback the optimization [110] (Figure 3c). It is expected that more machine learning, in particular generative neural networks, will be adapted in nanoparticle synthesis workflow in future for designing application-tailored nanoparticles in a variety of disciplines, such as medicine, energy, and more.

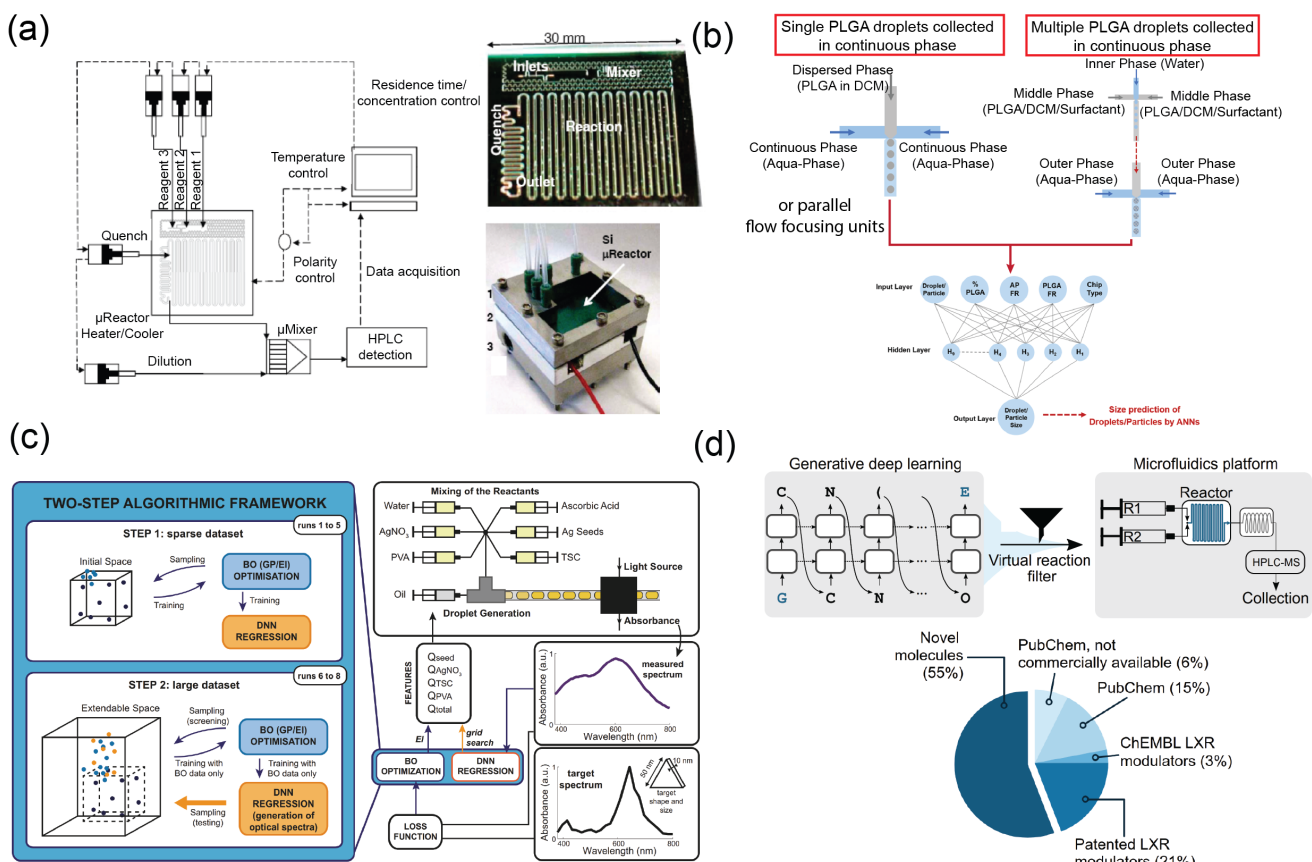


**Figure 3.** Microfluidics integrated with machine learning for process optimization and drug discovery. (a) An automated microfluidic system for automated optimization of chemical synthesis. Reprinted with permission from [103]. Copyright 2010 American Chemical Society. The font size have been adjusted for sake of clarity. (b) A droplet microfluidic platform combined with AI for synthesizing poly(Lactide-co-glycolide) (PLGA) microparticles from precipitating out of dichloromethane (DCM) [119]. Reproduced under CC-BY license. The figure has been reproduced for sake of clarity. (c) Two-step drug synthesis microfluidic platform with machine learning optimization [110]. Reproduced under CC-BY license. (d) A micromixer microfluidic platform combined with generative AI for de novo drug design and synthesis [121]. Reproduced under CC BY-NC (noncommercial) license.

### 3.3. Drug Development

The automation and miniaturization capabilities of microfluidics make it a good candidate for drug synthesis, drug delivery, formulation, and susceptibility testing [122,123]. Here, we discuss the integration of AI with microfluidics for drug design, synthesis, and formulation. The susceptibility testing application is discussed later in the following section.

Reinforcement learning provides an *in silico* means to generatively iterate drug design based on input physicochemical properties. Popova et al. utilized such an approach to create novel chemical libraries where the neural network can design chemicals by varying physical properties [124]. Recently, Grisoni et al. took a similar approach to generatively design drugs and further integrate with a microfluidic platform to synthesize the agonists against the liver X receptor [121] (Figure 3d). Such an automated platform combining AI and microfluidics introduces a closed-loop iterative optimization of drug design and synthesis that reduces human intervention. In the future, the improvement of algorithms with active learning could refine and optimize the design and synthesis process continuously. Similarly, machine learning used for iterating polymer synthesis and data-driven evaluation can accelerate drug formulation development [125].

## 4. Micro-Total Analysis System ( $\mu$ TAS) and Clinical Diagnostics

One major application of microfluidics is the automation of chemical analysis and clinical diagnostics, especially for point-of-care testing (POCT) [126,127]. In lab-on-chip technologies, various experimental processes are integrated and miniaturized onto a single microfluidic chip [128]. Further enhancement of data analysis and exclusion of potential human prejudice by integrating AI sets a feasible path toward realization of a  $\mu$ TAS [129].

### 4.1. Disease Diagnosis and Prognosis

To monitor human physiological status, detection and quantification of biomarkers using calibrated biosensors are required. Although conventional quantification by interpolation with a reference is standardized, utilization of AI to quantify and detect anomalies from pattern recognition in long-term clinical data presents unique opportunities. Combining paper microfluidics and ANN, the glucose concentration presented by the colorimetric method can be quantified and calibrated with high accuracy, as demonstrated in artificial urine and saliva [130,131].

Moreover, sensing applications based on image classification and recognition are particularly suitable for machine learning methods. Munoz et al. reported a machine learning method to detect label-free DNA based on fractal structures in subnanoliter droplets after loop-mediated isothermal amplification (LAMP) [132]. Similarly, optical detection of debris containing ambient RNA in droplets and excluded in data preprocessing can improve the data quality for single-nucleus RNA sequencing by using a semisupervised machine learning technique [133]. Alternatively, machine learning algorithms can also be applied to electrical inference of size and detection of ultrafine particles with low mean error [134].

Machine learning algorithms are sensitive to changes in cellular optical features due to biophysical properties or protein deformation. AI-enhanced microscopic image analysis of cells and tissues, therefore, is used for disease diagnosis in clinical settings. Deep-learning-assisted classification of the adhesion and deformation of RBCs in microchannels can be used to diagnose and monitor sickle cell anemia [135–137]. Rizzuto et al. combined microfluidics and AI-based video analysis to classify RBCs after passing microfluidic constrictions for diagnosis of hereditary hemolytic anemia [138]. The neural network can also predict the rigidity of RBCs directly from brightfield microscopy images. Ellett et al. used a microfluidic device to quantify the mobility of neutrophils in whole blood in combination with machine-learning-based scoring for diagnosis of sepsis with 97% and 98% sensitivity and specificity [139].

Similarly, rapid classification and quantification of cancer cells in various tissues and bodily fluids can be accelerated by AI in the fields of liquid biopsy or digital pathology, aiding clinicians and clinical laboratory scientists in disease diagnosis and prognosis, such as in leukemia, prostate, breast, brain, and lung cancers [140–145]. Many cells shed from primary tumors into patients' circulatory systems in the form of circulating tumor cells (CTCs). The amount of CTCs in patients' blood, even after treatments, correlates with the prognosis, also known as minimum residual disease (MRD). Therefore, concentration of CTCs is a novel biomarker for cancer management. The presence of CTCs can be analyzed and can predict prognosis with the aid of AI [146,147].

Mainstream immunochemical biosensors utilize the recognition ability of antibodies to detect and quantify biomarkers in various bodily fluids. Integrated with microfluidics, McRae et al. developed a compact programmable bionanochip platform (pBNC) on which multiplex immunoassays against prostate cancer, ovarian cancer, acute myocardial infarction, and drugs of abuse were performed on disposable cartridges for POCT applications. Afterward, the data were relayed to machine learning algorithms for further diagnosis based on previously trained data (Figure 4a) [148–150]. Furthermore, optical-based immunoassay readout can be resolved with the aid of machine learning. Song et al. reported a digital-enzyme-linked immunosorbent assay (ELISA) microarray for multiplex quantification of cytokines in patients who underwent cancer therapy [151] (Figure 4b). The turnaround time of the 12-plex assay was within 40 min by taking advantage of the microwell-based microarray and automated AI image analysis for biomarker quantification.

Immunochemical methods, however, suffer limitations such as interference to ligand-antibody interaction and the concentration-dependent hook effect, limiting the sensitivity, specificity, and linear range of detection [152]. Utilizing machine learning algorithms has also been shown to drastically improve the assay specificity and quantification of very high target concentration in surface-enhanced Raman spectrometric immunoassay and particle agglutination immunoassay [153–155].

In recent decades, the use of microfluidics for clinical testing has seen much growth due to increased adaption of POCT. At the same time, deep learning methods spur rapid development of AI across broad disciplines and applications. Humankind then met the challenge of a global pandemic at a scale not seen since the 1918 Spanish flu, the coronavirus disease 2019 (COVID-19), caused by severe acute respiratory syndrome coronavirus 2 (SARS-CoV-2) [156,157]. The rapid spread of the disease came with devastating consequences where healthcare systems were stretched to limits, state economies were stalled, and social norms were disrupted. Microfluidics was quickly adapted to develop quick turnaround of immunological as well as molecular antigen tests for rapid identification and diagnosis of exposed citizens and patients [158–160] for subsequent quarantine to curb the spread of the infectious disease. For example, Bhuiyan et al. developed an AI-controlled programmable microfluidic platform to perform ELISA immunoassays for cardiovascular disease diagnosis and SARS-CoV-2 diagnosis [161,162]. Many microfluidic POCT sensing platforms are also integrated with AI for analysis. Combining information and communication technologies (ICTs) with microfluidics, such as interfacing a smartphone with POCT devices, provide a solution for rapid testing in low-resource settings where gold-standard molecular diagnostics may not be easily available [163–166].

The combination of rapid testing offered by microfluidics and automated data analysis by AI has immense potential for proactive management of emerging infectious diseases. Not only can new diagnostics tests be rapidly developed after identification of antigen for future emerging infectious disease, but development of vaccines and drugs could be accelerated as well, through automation by microfluidics and AI [167–170].

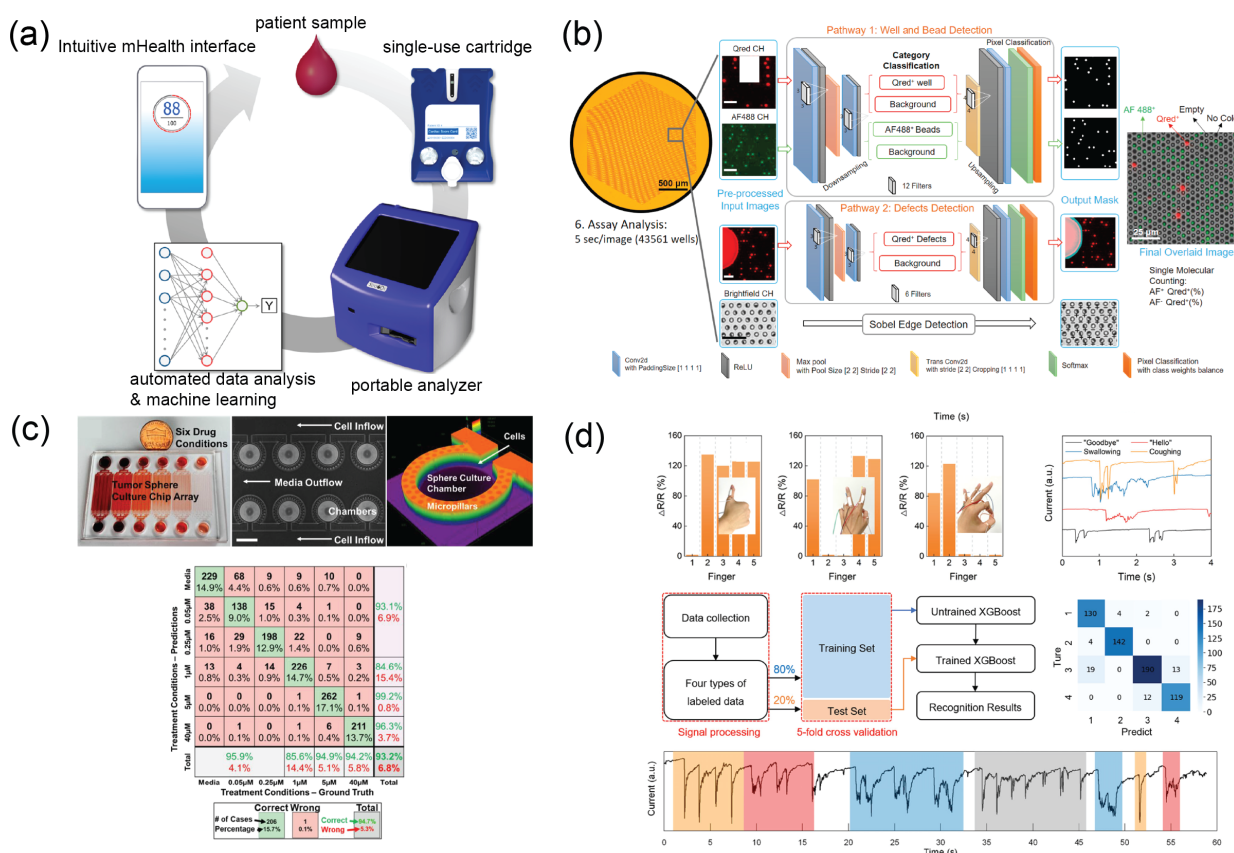


**Figure 4.** Micro- total analysis systems integrated with machine learning for clinical diagnostics. **(a)** A compact programmable microfluidic platform capable of performing multiplex immunoassay for POCT applications. Reprinted with permission from [150]. Copyright 2016 American Chemical Society. **(b)** A digital ELISA microarray for cytokine quantification with CNN-guided image processing. Reprinted with permission from [151] with permission from Elsevier. **(c)** A microfluidic platform with a convolutional neural network to predict drug efficacy based on the viability of cultured cancer spheres. Reprinted with permission from [171]. Copyright 2019 American Chemical Society. **(d)** A wearable sensor platform with AI data analysis for motion classification [172]. Reproduced under CC-BY license.

#### 4.2. Drug Susceptibility Testing

Integrated microsystems can not only isolate target cells for analysis, but they also integrate with mixing functions to investigate the susceptibility of target cells to pharmaceutical agents, an important parameter for clinical decisions. One common application is the liquid biopsy. Kobayashi et al. showed that by combining microfluidic flow cytometry, time-stretch microscopy, and machine learning enables high-throughput, label-free analysis drug susceptibility of breast cancer, leukemia cells, and platelets in as little as a 500  $\mu$ L sample [173–175].

Other major applications for drug susceptibility testing in clinical settings are therapeutic drug monitoring (TDM) and antimicrobial susceptibility testing (AST), where AI algorithms have begun to be adapted for monitoring and prediction [176,177]. Particularly for conventional AST, the time-to-result is of the essence for patient care. Therefore, automated microfluidic platforms in conjunction with optical detection and deep learning-powered analysis to rapidly detect bacteria, as well as screening and identifying appropriate antibiotics choices and therapeutic ranges, are driven by clinical needs [178–181].

Three-dimensional tissue models such as spheroids have the potential of mimicking tissue heterogeneity and drug transport in the microenvironment of an organism. However, 3D tissues have poor optical transmission in the visible light regions, making optical

characterization and evaluation difficult, especially for conventional computer vision algorithms. Deep learning models learn the features of target structures through pattern recognition in images; therefore, they have great potential in image analysis for 3D tissue images. Zhang et al. developed an automatic microfluidic chip in combination with CNN-based image screening for evaluating drug susceptibility through viability prediction of tumor spheres (Figure 4c) [171]. The effective drug changes the morphology and optical quality of the spheroids, and AI models learn to associate the image with phenotypic results. Therefore, the AI models are capable of predicting phenotype based on label-free images. The trainability and predictive potential of deep learning in combination with microfluidic drug testing platform could be a promising alternative to animal testing [182].

#### 4.3. Smart Wearables

Microsystems engineered through semiconductor processes are often rigid; therefore, they are limited from conformal sampling on organisms despite portability. When lab-on-chip systems are engineered on flexible substrates such as silicone or polyimides, such wearable microsystems enable long-term seamless biosampling and measurements [126] where conventional medical devices are often limited. Zhang and Tao showed that soft electrical sensors adhered on skin in combination with machine learning enabled long-term electrophysiological measurements [183]. In the management of cardiovascular diseases, early detection of abnormal electrical signals empowered by AI also has tremendous interests [184]. Similar needs in long-term monitoring of glucose in diabetes mellitus (DM) patients could also benefit from the combination of wearable devices and machine learning to predict the onset of hyperglycemia on the fly [185,186].

Soft sensors attached to the human body permit the measurement of pressure, force, and strain to infer biomechanics. Machine learning algorithms can be used to calibrate sensors [187,188] as well as tracking and predicting human gaits and motions (Figure 4d) [172,189]. Joining a multitude of sensors with Internet connectivity with AI at the core of data analysis offers a promising future in personalized healthcare [190].

### 5. AI Approach for Quantitative Biology

Machine learning algorithms can discern patterns in complex and noisy biological data; therefore, advances have been made recently in the field of cell analysis and personalized medicine by adopting AI for quantitative biology [191].

#### 5.1. Cell Analysis

Counting, classifying, and sorting of cells are essential processes that have been long adopted in microfluidics and not only used in clinical diagnostics but also in basic research. Integration with AI further extends the data processing ability, such as prediction and pattern recognition for phenotype identification in cell data, which initiated a new era of intelligent microfluidics [192].

##### 5.1.1. Cell Counting and Classification

The number of suspended cells in a solution can be counted conventionally through optical detection, electrical resistance (Coulter method), or impedance [193]. Machine learning algorithms such as support vector machine (SVM), logistic regression, or ANN can extract cell features in optical images [194], lens-free holographic images [195], electrical data [196], or a combination of two [197] for counting and classification.

In combination with a brightfield or fluorescence microfluidic flow cytometer, cells can be counted, classified, and tracked at high speed using supervised learning as well as unsupervised learning models [198–202]. Heo et al. showed that a supervised learning pipeline combining a fully-connected regression network and CNN distinguished K562 leukemia cells and RBCs with mean average precision (mAP) as high as 93.3% at 500 FPS [198]. Deep learning models trained for virtually enhancing resolution can also be combined with

low-resolution, high-speed microfluidic flow cytometry for counting and classifying algae, mammalian cells, and yeasts [201].

Minute optical property differences in cells which are difficult to discern by the naked eye can be classified by machine learning algorithms after proper training. Rossi et al. showed that CD4 and CD8 T lymphocytes can be differentiated by their scattered light due to biophysical property differences [203]. Polarization microscopy can also be conjugated with machine learning for the detection and classification of non-small-cell lung cancer cells without any staining [204].

In quantitative phase imaging (QPI) techniques, phase differences contributed by differences in refractive index of various cellular components can be quantified using digital holographic microscopy [205], lens-free holographic microscopy [206], interferometry [207,208], or time-stretched microscopy [209], both in 2D and 3D [210]. Conventional algorithms for phase retrieval are often time-consuming because image data can be noisy. Using machine learning, optical properties such as absorption, scattering, and refractive indexes can be used to extract biophysical information of cells such as dry mass. Without any labeling, only minute differences exist between nucleated white blood cells (WBCs) and cancer cells. Hirotsu et al. demonstrated that deep learning can assist label-free identification of cancer cells from WBCs, with the area under the curve of receiving operating characteristics (ROCs) reaching 95.7% [208]. Especially in time-stretched microscopy, broadband optical pulses image cells without any label at extremely high frame rates through photodiode readout and reconstruction [211–215]. Leukemia cells, RBCs, algae, and platelets can be classified by CNNs at extremely high flow speed ( $>10,000$  cells per second) inside microfluidic flow cytometry with high accuracy ( $>96\%$ ) [216]. High-speed, time-stretched imaging can also couple with high-speed microfluidic cell classification and real-time label-free electrostatic cell sorting enabled by powerful GPU processing (Figure 5a) [213].

Electrodes can readily be fabricated with microfluidic channels and used for detection of cells by resistance or impedance detection. Machine learning algorithms can be further integrated into data analysis to classify objects based on their resistance or impedance characteristics [217–221]. Joshi et al. combined ink-jet printed microfluidics with machine learning algorithms to classify and differentiate three types of cancer cells based on their impedance profiles [217]. A deep learning algorithm with closed-loop feedback can regulate precise cell impedance measurement and classification [219]. Similarly, Feng et al. combined a microfluidic impedance flow cytometry with machine learning, showing capability of classifying five different cancer cells based on their membrane capacitance, cytoplasm, conductivity, and radius, with an accuracy of 91.5% [220].

### 5.1.2. Cell Sorting

Flow cytometry is a cornerstone for high-throughput single cell classification with applications across clinical diagnostics and basic biomedical research. Further coupling the selection function for interested target populations provide many downstream applications, such as single cell molecular analysis, immunoassay, and selective cultivation [222].

Machine-learning-powered cell classification in brightfield and fluorescence flow cytometry can be integrated with a microfluidic flow cell with piezoelectric or pneumatic actuators to hydrodynamically collect cells or droplets of interest from classification in real time [97,223–225]. By adapting lightweight CNNs, high-speed electronics, and GPUs, real-time image classification and precise timing control for cell sorting have been realized. Aforementioned ultrahigh-speed QPI imaging systems integrated with sorting functions have been demonstrated, reaching accuracy above 94% at 100 events per second [226–228] (Figure 5b). By using machine learning to classify sperm and predict their DNA fragmentation index, a sperm sorter was developed that has broad applications in fertility medicine as well as in the veterinary industry [229].

Other cell sorting methods, such as magnetic sorting and dielectrophoretic cell sorting, have also been reported to integrate machine learning [230,231]. In particular, magnetic immunoseparation is a well-adapted concentration and purification method for clinical

diagnostics as well as biotechnology. Uslu et al. showed that SVM algorithms can assist identification of leukemia cells captured with light-obstructing magnetic particles with a precision of 91.6% under  $40\times$  objective [230]. Moreover, magnetic particles are often hard to remove completely after the sorting is completed. By using machine learning for image analysis and classification, the residual amount of magnetic particles can also be quantified.

### 5.1.3. Cell Phenotype Analysis

The possibility of deep learning is demonstrated by its ability to extract the features related to minute optical differences contributed by biological microstructures. Fluorescence images of subcellular structures can be predicted with CNNs from cell images taken under brightfield microscopy without any staining [232–234]. Style transfer from one staining to another staining is also proven [235]. Such *in silico* labeling can also be applied to high-speed QPI-based microfluidic flow cytometry [236]. Moreover, deep learning methods have demonstrated high-quality segmentation, and they can further extract features regarding phenotypes.

The mechanical deformability and relaxation of cells can be probed by microfluidic shear flow or microstructure constriction [237–239]. By further applying analysis empowered with machine learning, the mechanical properties of cells can be predicted from optical images with accuracy reaching over 90% [137,240].

The health state of cells in microfluidic platforms for drug screening can also be predicted and have vast applications in drug susceptibility testing, immunotherapy efficacy testing, and drug resistance monitoring [241–243]. For example, to maintain cellular homeostasis, the timing and frequency of cellular metabolism, DNA duplication, and division are tightly regulated in the cell cycle in four phases: gap 1 (G1), synthesis (S), gap 2 (G2), and mitosis (M). Conventionally, identification of the cell cycle requires staining of cells against molecular markers for nucleic acid and various essential proteins for DNA replication [244]. By training CNNs on training data annotated from fluorescence information, the CNNs can be used to classify cell cycles and even predict them in brightfield images [245–248]. With the combination of microfluidic trapping, such a platform can have broad applications for predicting cell cycle phenotypes in drug screening and basic research [249,250]. Aspert et al. used microfluidic and deep learning for high-throughput tracking of single cell division and emergence of mutants [250] (Figure 5c). By adapting deep learning, analysis of the survival and phenotype changes of large amounts of single cell data could be automated, greatly saving time, minimizing human bias, and increasing statistical power.

Cellular senescence upon exposure to reactive oxygen species, a key contributor to aging, is also a phenotype that requires quantification by staining, typically against senescence-associated beta-galactosidase activity. CNNs have also been demonstrated to predict cellular senescence based on the morphology or optical quality of the cell in brightfield [251,252]. By expanding the AI for phenotype prediction, cellular phenotypes in biomimetic microenvironments established by microfluidics have broad potential applications.

### 5.1.4. Spatiotemporal Cellular Dynamics Analysis

Deep learning methods, especially CNNs, are particularly effective in image segmentation across brightfield and fluorescence microscopy, outperforming conventional computer vision methods [253–255]. Accurate segmentation accompanied by precise tracking enables the accurate analysis of complex cellular dynamics in a stack of timelapse images and contributes to quantitative understanding of cellular processes. For example, Bove et al. used CNN classification and Bayesian inference tracking for understanding the role of cell competition in epithelial tissue maintenance [256]. Accurate segmentation by deep learning also benefits tracking cell migration in both 2D and 3D [257–260].

Through coupling with microfluidics, cellular dynamics can be studied in detail in dedicated microenvironments compatible with high-resolution imaging. Single bacterium

evolution and bacteria population dynamics can be experimentally modeled on microfluidic devices and analyzed using machine learning models [261–264].

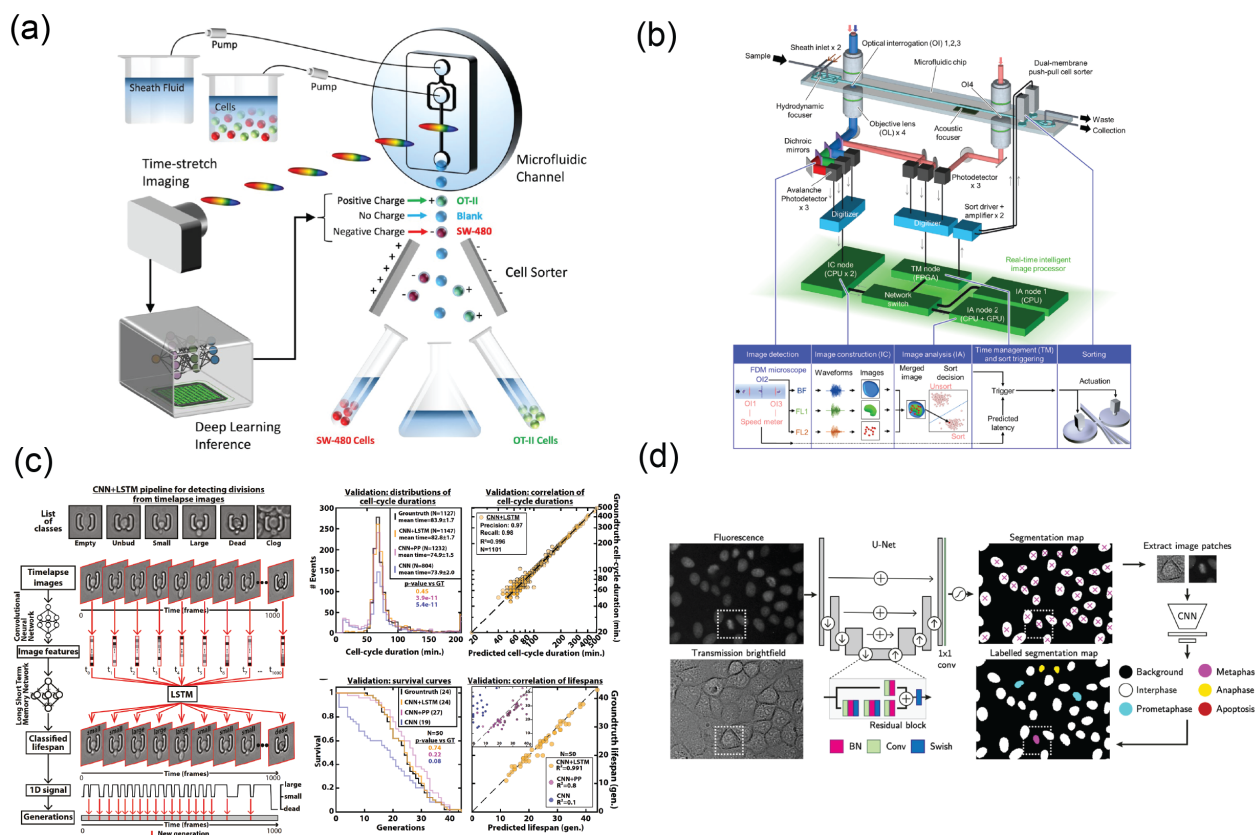


**Figure 5.** Microsystems integrated with AI for cell analysis. **(a)** An optofluidic time-stretch QPI cell sorter based on high-speed, label-free cell classification and sorting empowered by deep learning [213]. Reproduced under CC-BY license. **(b)** Frequency-multiplexed microscopy coupled with real-time machine learning processing and piezoelectric actuator for high-speed cell sorting. Reprinted from [226] with permission from Elsevier. **(c)** A microfluidic cell trap with AI phenotype prediction for yeast division tracking and survival analysis [250]. Reproduced under CC-BY license. **(d)** A deep learning framework to automatically classify cell cycles and track lineage trees [265]. Reproduced under CC-BY license.

Wang et al. used a deep learning-based segmentation with Bayesian filtering to track migration of cells of a 3D angiogenic vessel with an accuracy of 86.4% [266]. Cell migration guided by physical or chemical gradients can be studied with high-throughput microfluidic platforms, while AI-empowered tracking relieves humans from the tedious task. Quantification of cell migration and growth kinetics can be analyzed with reduced risk of human bias [267,268]. Furthermore, accurate cell tracking across multiple cell divisions enables building of lineage trees, and is capable of revealing the population dynamic information of cells throughout the experimental period. Ulicna et al. combined residual U-net, CNN classification, and Bayesian tracking to reconstruct the cellular lineages in thousands of hours of timelapse data and identified cell cycling heterogeneity and correlated cyclings between cells of similar generation [265] (Figure 5d). Similar machine learning inference can also be applied to resolving temporal dynamics of multicellular organoids at single-cell level in 3D [269,270].

## 5.2. Personalized Medicine

Advances in quantitative biology in modern biomedical research spur the development of personalized medicine, a discipline where biological variation is recognized and tailored

care is aimed towards every individual [271]. Microfluidics and AI as an integrated solution has great potential and opportunity for personalized medicine.

Automated microfluidics and POCT devices can be deployed for dedicated patients for rapid turnaround of personalized molecular diagnostics results. Moreover, patient-derived cells, tissues, and induced pluripotent stem cells (iPSCs) can be incorporated on a microfluidic platform, also known as an organ-on-chip (OoC), recreating patient-specific multicellular microenvironments [272]. The OoC has broad potential, from being a clinical diagnostics vehicle to a personalized drug development tool as well as a fundamental biomedical research platform. By using human- or patient-derived cells and tissues, the results are more clinically translatable, and AI-empowered analysis can deliver prediction of prognosis and therapy outcome [273]. Furthermore, the OoC could potentially replace animal studies, resolving decades-long dilemmas in research ethics [274,275].

### 5.2.1. Integration with Molecular Bioinformatics

Microfluidic technologies have been adapted for genomics and transcriptomics studies, both in the core of the sequencing platform, such as sequencing flow cells of next-generation sequencing (NGS), and sample and library preparation, such as single cell isolation using droplet microfluidics [276,277]. Because many of the techniques use Poisson statistics, by adopting machine learning algorithms in bioinformatic pipelines, the quality of library preparation and data quality can be improved and helps advance multiomics studies such as spatial transcriptomics and metabolomics [191,278,279]. For example, Ko et al. applied nanofluidics and machine learning to predict cancer in mice and patients using exosomal mRNA profiles learned through linear discriminant analysis [280].

### 5.2.2. Organ-on-Chips as Human Mimetic Models

Organ-on-chips (OoCs) aim to recreate multicellular complex environments *in vitro* on microfluidic platforms to recapitulate the complex tissue interaction with physical and chemical gradients existing in the biological microenvironment [281]. Many OoCs adapting human-derived primary cells, stem cells, or cell lines have been developed for different organs models, such as brain [282,283], thyroid [284], heart [285], stomach [286], intestine [287], lungs [288,289], liver [290], kidneys [291], pancreas [292], and bladder [293].

The complexity of OoC platforms offers many opportunities for automation and data analysis, both of which can benefit a lot from AI [294]. In particular, when patient-specific tissues or iPSC-differentiated cells are used, OoCs have the potential to recapitulate the human physiology and deliver personalized medicine without the need for animal testing [295–297].

Due to the excellence in image segmentation and predictive potential, AI has started to be integrated with OoC platforms for image analysis, correlation, and prediction of clinical results. Paek et al. created a bone OoC as a drug-testing platform for osteoporosis. CNN-based image segmentation provided quantitative measurements of beta-catenin translocation to evaluate the efficacy of the osteoporosis suppressive antibody [298] (Figure 6a). Likewise, a blood–brain niche (BBN) chip was developed to model the extravasation of breast cancer cells into a brain-mimetic niche [299,300]. The invasion of cancer cells through an endothelial cell sheet was evaluated by confocal 3D tomography, and several machine learning algorithms were benchmarked to classify the metastatic potential of the cancer cells. The ANN was found to outperform other machine learning algorithms (Figure 6b). Chong et al. developed a microfluidic multicellular coculture array for testing skin sensitivity to drugs [301]. By combining SVM and principle component analysis on image results for several apoptosis markers, adverse cutaneous drug reactions can be predicted with the accuracy of 87.5% and the specificity of 75%. The predictive evaluation could have huge potential in personalized medicine to aid in preventing severe adverse reactions, such as Steven Johnson syndrome and toxic epidermal necrolysis syndrome.

Alternatively, a sheet of muscle cells placed on a microfluidic stretching platform can be quantitatively studied with the assistance of AI. Recurrent neural networks (RNNs) with

long short-term memory (LSTM) blocks were used to predict the subsequent dynamics of muscle cells from one time point in conjunction with a CNN to predict the phenotype of them [302] (Figure 6c).

The complexity of the immune-tumor niche also makes it a key topic suitable for combined approach by OoC and AI analysis [303]. The interaction between dendritic cells and leukocytes with cancer cells in a 3D microfluidic coculture platform can be accurately segmented and tracked with the aid of deep learning [304–307]. Nguyen et al. constructed an immune-competent OoC that reconstitutes cancer, immune, endothelial cells, and fibroblasts altogether for studying immune–tumor interactions and immunomodulation of cancer-associated fibroblasts [306] (Figure 6d). The synergy between OoC and AI shows a promising future of personalized medicine.

### 5.2.3. Personalized Drug Development

One key concept of personalized medicine is recognizing that individuals have biological variations both in biochemistry and drug responses [308]. Utilization of AI for personalized drug optimization by both drug selection and dosage has been promising [309,310]. A microfluidic POCT device for MRD and an OoC for tracking cancer migratory abilities were demonstrated for evaluation of patient-specific cancer drug efficacy by combining AI analysis [311,312]. It is expected that we will see more examples and applications combining microfluidic biomimetic models integrated with AI analysis and prediction in the future, such as integrated lab-on-chip devices for personalized diagnosis, medicine formation, and even drug delivery [313].

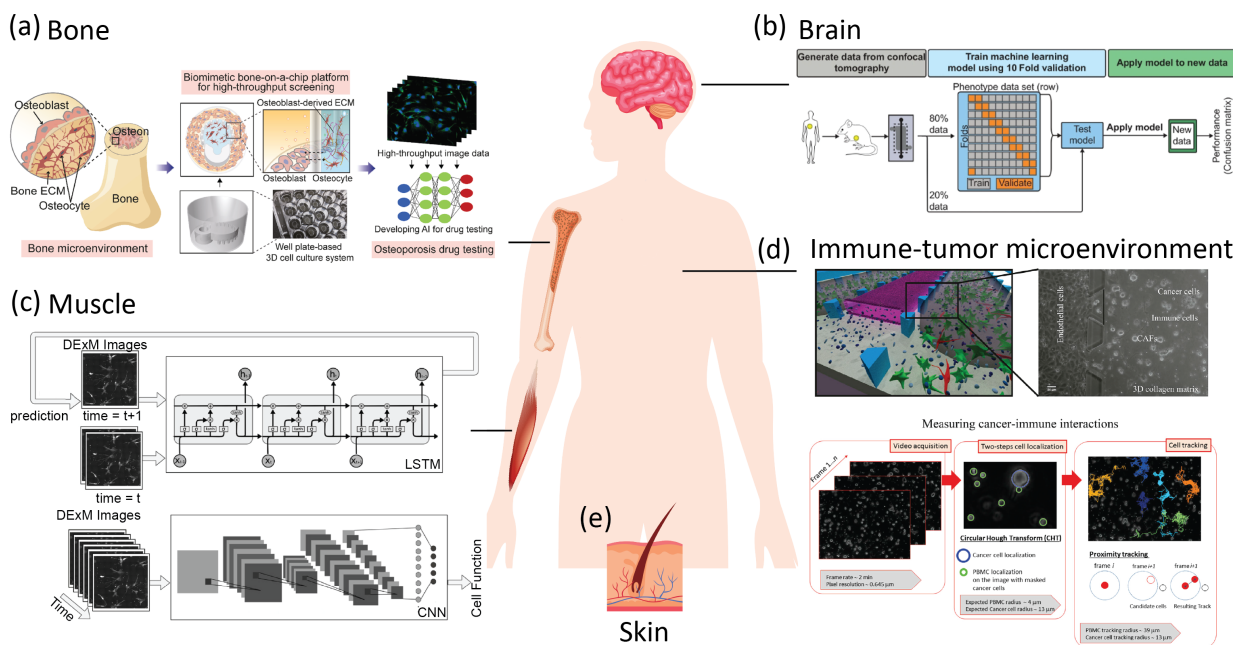


**Figure 6.** Organ-on-chip platforms integrated with AI analysis. (a) A bone-on-chip for osteoporosis drug testing and development [298]. Reproduced under CC-BY license. (b) A blood–brain niche OoC for predicting the metastatic probability of brain cancer [299,300]. Adapted with permission from [300]. (c) A muscle-on-chip with AI image analysis for quantitative understanding of muscular cell phenotypes. Reprinted with permission from [302]. (d) An OoC to reconstitute immunocompetent tumor microenvironment in breast cancer [305,306]. Reproduced under CC-BY license. (e) A skin-on-chip for predicting adverse cutaneous drug reactions [301]. Components in the figure were designed by macrovector; brgfx/Freepik.

## 6. Discussion and Outlook

Microfluidics is a rapidly advancing field that involves manipulating small fluid volumes at the microscale. One of the key challenges in this field is the ability to control and

analyze the complex fluid dynamics that occur on such a small scale. In recent years, there has been growing interest in integrating AI with microfluidics to address this challenge. AI has the potential to revolutionize microfluidics by enabling the development of intelligent control systems that can adapt to changing conditions in real-time. Additionally, AI-based image analysis techniques can automatically detect, classify, and track objects of interests in microfluidic systems, providing valuable insights as well as prediction of their dynamics. The integration of AI with microfluidics could lead to the development of more sophisticated lab-on-a-chip diagnostic devices, more efficient and effective drug delivery systems, and more versatile monitoring platforms. AI-empowered image analysis delivers quantitative analysis of cells and tissues in complex OoCs and opens a new era in quantitative biology and personalized medicine.

Overall, the advantages of integrating AI with microfluidics include automation, efficiency, and quantitative analysis in data processing, as well as cost effectiveness due to the low reagent consumption of microfluidics. AI can perform large-scale iterations and automation of planning and executing experimental parameters. The trainability of AI empowered it to flexibly learn from data and predict even when a priori annotation is not always available. The neural networks especially outperform conventional algorithms in image and language recognition, which are often abundant in biomedical and clinical data, opening possibilities to automate quantitative analysis of data that was conventionally difficult to analyze.

However, some challenges must be addressed. Firstly, robust AI algorithms and reliable data inputs are necessary for successful integration. While recent advancements have demonstrated the power of AI algorithms, they are often considered a “black-box” due to their lack of explainability. To build trustworthy AI-integrated microfluidic systems, it is crucial to prioritize explainability and validation because quality assurance and risk management are of the utmost importance in medical instrumentation. Secondly, AI operations can be computationally expensive; both training and inference demand immense parallel processing power. Therefore, energy efficiency and deployability for particular applications and their environments are essential. For example, when integrating with a microfluidic POCT system in a low-resource setting, such as a rural area with intermittent power supply, a lightweight AI on an edge computing platform may be crucial for successful integration. Additionally, data size is a critical factor in AI performance, which scales proportionally with the amount of the data. While combining the automation capability of microfluidics and MEMS with data from existing methods for training AI systems can be challenging, data fusion could provide a unified and comprehensive dataset that enables AI systems for more reliable predictive analysis. Cooperation within the scientific community for data sharing and training AI systems with federated learning can also address the challenges of both explainability and deployability.

In summary, by integrating the compact and versatile microfluidic platforms with the intelligent control and analysis with AI, we expect new breakthroughs in healthcare in the near future, but caveats must be taken to validate the AI system for any applications and evaluate potential risks.

**Author Contributions:** Conceptualization, S.P. and H.-F.T.; writing—original draft preparation, S.P., P.-Y.C. and H.-F.T.; writing—review and editing, H.-F.T.; supervision, H.-F.T.; funding acquisition, H.-F.T. All authors have read and agreed to the published version of the manuscript.

**Funding:** This research was funded by National Science and Technology Council, Taiwan under grant number NSTC 111-2222-E-182-004.

**Data Availability Statement:** No new data were created or analyzed in this study.

**Conflicts of Interest:** The authors declare no conflict of interest.

## Abbreviations

The following abbreviations are used in this manuscript:

AI	Artificial Intelligence
AIV	Artificial Intelligence Velocimetry
ANN	Artificial Neural Network
AST	Antimicrobial Susceptibility Testing
CC-BY	Creative Commons Attribution 4.0 License
CFD	Computational Fluid Dynamics
CNN	Convolutional Neural Network
CTC	Circulating Tumor Cells
DM	Diabetes Mellitus
ELISA	Enzyme-Linked ImmunoSorbent Assay
FPS	Frames Per Second
GPU	Graphics Processing Unit
ICT	Information and Communication Technology
iPSC	Induced Pluripotent Stem Cell
IR	Infrared
LAMP	Loop-mediated isothermal AMPlification
MEMS	Microelectromechanical systems
MRD	Minimum Residual Disease
μTAS	Micro-Total Analysis System
OoC	Organ-on-Chip
POCT	Point-Of-Care Testing
QPI	Quantitative Phase Imaging
RBC	Red Blood Cell
RNN	Recurrent Neural Network
SNR	Signal-to-Noise Ratio
SVM	Support Vector Machine
TDM	Therapeutic Drug Monitoring
WBC	White Blood Cell
YOLO	You Only Look Once

## References

- Whitesides, G.M. The origins and the future of microfluidics. *Nature* **2006**, *442*, 368–373. [[CrossRef](#)] [[PubMed](#)]
- Stone, H.A. Introduction to Fluid Dynamics for Microfluidic Flows. In *CMOS Biotechnology*; Lee, H.; Westervelt, R.M.; Ham, D., Eds.; Series on Integrated Circuits and Systems; Springer: Boston, MA, USA, 2007; pp. 5–30.
- deMello, A.J. Control and detection of chemical reactions in microfluidic systems. *Nature* **2006**, *442*, 394–402. [[CrossRef](#)] [[PubMed](#)]
- Velve-Casquillas, G.; Le Berre, M.; Piel, M.; Tran, P.T. Microfluidic tools for cell biological research. *Nano Today* **2010**, *5*, 28–47. [[CrossRef](#)] [[PubMed](#)]
- Liu, Y.; Jiang, X. Why microfluidics? Merits and trends in chemical synthesis. *Lab Chip* **2017**, *17*, 3960–3978. [[CrossRef](#)] [[PubMed](#)]
- Nielsen, J.B.; Hanson, R.L.; Almughamsi, H.M.; Pang, C.; Fish, T.R.; Woolley, A.T. Microfluidics: Innovations in Materials and Their Fabrication and Functionalization. *Anal. Chem.* **2020**, *92*, 150–168. [[CrossRef](#)]
- Jordan, M.I.; Mitchell, T.M. Machine learning: Trends, perspectives, and prospects. *Science* **2015**, *349*, 255–260. [[CrossRef](#)]
- Uhrig, R. Introduction to artificial neural networks. In Proceedings of the IECON '95-21st Annual Conference on IEEE Industrial Electronics, Orlando, FL, USA, 6–10 November 1995; Volume 1, pp. 33–37. [[CrossRef](#)]
- Schmidhuber, J. Deep learning in neural networks: An overview. *Neural Netw.* **2015**, *61*, 85–117. [[CrossRef](#)]
- Bishop, C.M. Neural networks and their applications. *Rev. Sci. Instrum.* **1994**, *65*, 1803–1832. [[CrossRef](#)]
- Ben-Nun, T.; Hoefer, T. Demystifying Parallel and Distributed Deep Learning: An In-depth Concurrency Analysis. *ACM Comput. Surv.* **2019**, *52*, 65:1–65:43. [[CrossRef](#)]
- Rao, Q.; Frtunekj, J. Deep learning for self-driving cars: Chances and challenges. In Proceedings of the 1st International Workshop on Software Engineering for AI in Autonomous Systems (SEFAIS '18), Gothenburg, Sweden, 28 May 2018; Association for Computing Machinery: New York, NY, USA, 2018; pp. 35–38. [[CrossRef](#)]
- Johnson, J. Artificial intelligence & future warfare: Implications for international security. *Def. Secur. Anal.* **2019**, *35*, 147–169. [[CrossRef](#)]
- Yu, T.C.; Chou, W.C.; Yeh, C.Y.; Yang, C.K.; Huang, S.C.; Tien, F.M.; Yao, C.Y.; Cheng, C.L.; Chuang, M.K.; Tien, H.F.; et al. Automatic Bone Marrow Cell Identification and Classification By Deep Neural Network. *Blood* **2019**, *134*, 2084. [[CrossRef](#)]

15. Lu, M.Y.; Williamson, D.F.K.; Chen, T.Y.; Chen, R.J.; Barbieri, M.; Mahmood, F. Data-efficient and weakly supervised computational pathology on whole-slide images. *Nat. Biomed. Eng.* **2021**, *5*, 555–570. [CrossRef] [PubMed]
16. Chen, C.L.; Chen, C.C.; Yu, W.H.; Chen, S.H.; Chang, Y.C.; Hsu, T.I.; Hsiao, M.; Yeh, C.Y.; Chen, C.Y. An annotation-free whole-slide training approach to pathological classification of lung cancer types using deep learning. *Nat. Commun.* **2021**, *12*, 1193. [CrossRef] [PubMed]
17. Podder, S.; Bhattacharjee, S.; Roy, A.; Podder, S.; Bhattacharjee, S.; Roy, A. An efficient method of detection of COVID-19 using Mask R-CNN on chest X-Ray images. *AIMS Biophys.* **2021**, *8*, 281–290. [CrossRef]
18. Galan, E.A.; Zhao, H.; Wang, X.; Dai, Q.; Huck, W.T.S.; Ma, S. Intelligent Microfluidics: The Convergence of Machine Learning and Microfluidics in Materials Science and Biomedicine. *Matter* **2020**, *3*, 1893–1922. [CrossRef]
19. Bai, Y.; Gao, M.; Wen, L.; He, C.; Chen, Y.; Liu, C.; Fu, X.; Huang, S. Applications of Microfluidics in Quantitative Biology. *Biotechnol. J.* **2018**, *13*, 1700170. [CrossRef]
20. McIntyre, D.; Lashkaripour, A.; Fordyce, P.; Densmore, D. Machine learning for microfluidic design and control. *Lab Chip* **2022**, *22*, 2925–2937. [CrossRef]
21. Renner, G.; Ekárt, A. Genetic algorithms in computer aided design. *Comput.-Aided Des.* **2003**, *35*, 709–726. [CrossRef]
22. Oh, K.W.; Lee, K.; Ahn, B.; Furlani, E.P. Design of pressure-driven microfluidic networks using electric circuit analogy. *Lab Chip* **2012**, *12*, 515–545. [CrossRef]
23. Xu, H.; Liu, R.; Choudhary, A.; Chen, W. A Machine Learning-Based Design Representation Method for Designing Heterogeneous Microstructures. *J. Mech. Des.* **2015**, *137*. [CrossRef]
24. Bhargava, K.C.; Thompson, B.; Iqbal, D.; Malmstadt, N. Predicting the behavior of microfluidic circuits made from discrete elements. *Sci. Rep.* **2015**, *5*, 15609. [CrossRef] [PubMed]
25. Tsur, E.E. Computer-Aided Design of Microfluidic Circuits. *Annu. Rev. Biomed. Eng.* **2020**, *22*, 285–307. [CrossRef] [PubMed]
26. Lore, K.G.; Stoecklein, D.; Davies, M.; Ganapathysubramanian, B.; Sarkar, S. Hierarchical Feature Extraction for Efficient Design of Microfluidic Flow Patterns. In Proceedings of the 1st International Workshop on Feature Extraction: Modern Questions and Challenges at NIPS2015, Montreal, Canada, 11 December, 2015; PMLR: Cambridge, MA, USA, 2015; pp. 213–225.
27. Stoecklein, D.; Lore, K.G.; Davies, M.; Sarkar, S.; Ganapathysubramanian, B. Deep Learning for Flow Sculpting: Insights into Efficient Learning using Scientific Simulation Data. *Sci. Rep.* **2017**, *7*, 46368. [CrossRef]
28. Lee, X.Y.; Balu, A.; Stoecklein, D.; Ganapathysubramanian, B.; Sarkar, S. Flow Shape Design for Microfluidic Devices Using Deep Reinforcement Learning. *arXiv* **2018**. [CrossRef]
29. Granados-Ortiz, F.J.; Ortega-Casanova, J. Machine learning-aided design optimization of a mechanical micromixer. *Phys. Fluids* **2021**, *33*, 063604. [CrossRef]
30. Wang, J.; Zhang, N.; Chen, J.; Su, G.; Yao, H.; Ho, T.Y.; Sun, L. Predicting the fluid behavior of random microfluidic mixers using convolutional neural networks. *Lab Chip* **2021**, *21*, 296–309. [CrossRef]
31. Maionchi, D.d.O.; Einstein, L.; dos Santos, F.P.; de Souza Júnior, M.B. Computational fluid dynamics and machine learning as tools for optimization of micromixers geometry. *Int. J. Heat Mass Transf.* **2022**, *194*, 123110. [CrossRef]
32. Zhang, N.; Liu, Z.; Wang, J. Machine-Learning-Enabled Design and Manipulation of a Microfluidic Concentration Gradient Generator. *Micromachines* **2022**, *13*, 1810. [CrossRef] [PubMed]
33. Balabanov, A.V.; Kasimov, A.M.; Popov, A.I.; Fateev, V.Y. MNM-Modelling and Creating Designs of Discrete Microfluidics. In Proceedings of the 2021 14th International Conference Management of Large-Scale System Development (MLSD), Moscow, Russian, 27–29 September 2021; pp. 1–4. [CrossRef]
34. Lashkaripour, A.; Rodriguez, C.; Mehdipour, N.; Mardian, R.; McIntyre, D.; Ortiz, L.; Campbell, J.; Densmore, D. Machine learning enables design automation of microfluidic flow-focusing droplet generation. *Nat. Commun.* **2021**, *12*, 25. [CrossRef]
35. Shahab, M.; Rengaswamy, R. Reinforcement-Learning designs droplet microfluidic networks. *Comput. Chem. Eng.* **2022**, *161*, 107787. [CrossRef]
36. Haward, S.J.; Oliveira, M.S.N.; Alves, M.A.; McKinley, G.H. Optimized Cross-Slot Flow Geometry for Microfluidic Extensional Rheometry. *Phys. Rev. Lett.* **2012**, *109*, 128301. [CrossRef] [PubMed]
37. Wang, J.; Liang, K.; Zhang, N.; Yao, H.; Ho, T.Y.; Sun, L. Automated calibration of 3D-printed microfluidic devices based on computer vision. *Biomicrofluidics* **2021**, *15*, 024102. [CrossRef] [PubMed]
38. Shchanikov, S.; Zuev, A.; Bordanov, I.; Danilin, S.; Lukoyanov, V.; Korolev, D.; Belov, A.; Pigareva, Y.; Gladkov, A.; Pimashkin, A.; et al. Designing a bidirectional, adaptive neural interface incorporating machine learning capabilities and memristor-enhanced hardware. *Chaos Solitons Fractals* **2021**, *142*, 110504. [CrossRef]
39. Bachratý, H.; Bachratá, K.; Chovanec, M.; Jančigová, I.; Smiešková, M.; Kovalčíková, K. Applications of machine learning for simulations of red blood cells in microfluidic devices. *BMC Bioinform.* **2020**, *21*, 90. [CrossRef] [PubMed]
40. Zhang, N.; Liang, K.; Liu, Z.; Sun, T.; Wang, J. ANN-Based Instantaneous Simulation of Particle Trajectories in Microfluidics. *Micromachines* **2022**, *13*, 2100. [CrossRef]
41. Ahmed, F.; Shimizu, M.; Wang, J.; Sakai, K.; Kiwa, T. Optimization of Microchannels and Application of Basic Activation Functions of Deep Neural Network for Accuracy Analysis of Microfluidic Parameter Data. *Micromachines* **2022**, *13*, 1352. [CrossRef] [PubMed]
42. Kutz, J.N. Deep learning in fluid dynamics. *J. Fluid Mech.* **2017**, *814*, 1–4. [CrossRef]

43. Brunton, S.L.; Noack, B.R.; Koumoutsakos, P. Machine Learning for Fluid Mechanics. *Annu. Rev. Fluid Mech.* **2020**, *52*, 477–508. [[CrossRef](#)]
44. Kochkov, D.; Smith, J.A.; Alieva, A.; Wang, Q.; Brenner, M.P.; Hoyer, S. Machine learning–accelerated computational fluid dynamics. *Proc. Natl. Acad. Sci. USA* **2021**, *118*, e2101784118. [[CrossRef](#)]
45. Cai, S.; Li, H.; Zheng, F.; Kong, F.; Dao, M.; Karniadakis, G.E.; Suresh, S. Artificial intelligence velocimetry and microaneurysm-on-a-chip for three-dimensional analysis of blood flow in physiology and disease. *Proc. Natl. Acad. Sci. USA* **2021**, *118*, e2100697118. [[CrossRef](#)]
46. Zeng, X.; Xue, C.D.; Chen, K.J.; Li, Y.J.; Qin, K.R. Deep-learning-assisted extraction of height-averaged velocity from scalar signal transport in a shallow microfluidic channel. *Microfluid. Nanofluidics* **2022**, *26*, 36. [[CrossRef](#)]
47. Chen, Q.; Deng, J.; Luo, G. Micromixing Performance and Residence Time Distribution in a Miniaturized Magnetic Reactor: Experimental Investigation and Machine Learning Modeling. *Ind. Eng. Chem. Res.* **2023**, *62*, 3577–3591. [[CrossRef](#)]
48. Sharma, H.; Das, G.; Samanta, A.N. ANN-based prediction of two-phase gas–liquid flow patterns in a circular conduit. *AIChE J.* **2006**, *52*, 3018–3028. [[CrossRef](#)]
49. Giri Nandagopal, M.S.; Selvaraju, N. Prediction of Liquid–Liquid Flow Patterns in a Y-Junction Circular Microchannel Using Advanced Neural Network Techniques. *Ind. Eng. Chem. Res.* **2016**, *55*, 11346–11362. [[CrossRef](#)]
50. Nandagopal, M.S.G.; Abraham, E.; Selvaraju, N. Advanced neural network prediction and system identification of liquid–liquid flow patterns in circular microchannels with varying angle of confluence. *Chem. Eng. J.* **2017**, *309*, 850–865. [[CrossRef](#)]
51. Desir, P.; Chen, T.Y.; Bracconi, M.; Saha, B.; Maestri, M.; Vlachos, D.G. Experiments and computations of microfluidic liquid–liquid flow patterns. *React. Chem. Eng.* **2019**, *5*, 39–50. [[CrossRef](#)]
52. Abbasi Moud, A. Recent advances in utility of artificial intelligence towards multiscale colloidal based materials design. *Colloid Interface Sci. Commun.* **2022**, *47*, 100595. [[CrossRef](#)]
53. Iverson, B.D.; Garimella, S.V. Recent advances in microscale pumping technologies: A review and evaluation. *Microfluid. Nanofluidics* **2008**, *5*, 145–174. [[CrossRef](#)]
54. Dressler, O.J.; Howes, P.D.; Choo, J.; deMello, A.J. Reinforcement Learning for Dynamic Microfluidic Control. *ACS Omega* **2018**, *3*, 10084–10091. [[CrossRef](#)]
55. Au, A.K.; Lai, H.; Utela, B.R.; Folch, A. Microvalves and Micropumps for BioMEMS. *Micromachines* **2011**, *2*, 179–220. [[CrossRef](#)]
56. Abe, T.; Oh-hara, S.; Ukita, Y. Adoption of reinforcement learning for the intelligent control of a microfluidic peristaltic pump. *Biomicrofluidics* **2021**, *15*, 034101. [[CrossRef](#)] [[PubMed](#)]
57. Abe, T.; Oh-hara, S.; Ukita, Y. Integration of reinforcement learning to realize functional variability of microfluidic systems. *Biomicrofluidics* **2022**, *16*, 024106. [[CrossRef](#)]
58. Shayan, M.; Bhattacharjee, S.; Song, Y.A.; Chakrabarty, K.; Karri, R. Toward Secure Microfluidic Fully Programmable Valve Array Biochips. *IEEE Trans. Very Large Scale Integr. (VLSI) Syst.* **2019**, *27*, 2755–2766. [[CrossRef](#)]
59. Hajmohammadi, M.R.; Alipour, P.; Parsa, H. Microfluidic effects on the heat transfer enhancement and optimal design of microchannels heat sinks. *Int. J. Heat Mass Transf.* **2018**, *126*, 808–815. [[CrossRef](#)]
60. Miralles, V.; Huerre, A.; Malloggi, F.; Jullien, M.C. A Review of Heating and Temperature Control in Microfluidic Systems: Techniques and Applications. *Diagnostics* **2013**, *3*, 33–67. [[CrossRef](#)]
61. Rizkin, B.A.; Popovich, K.; Hartman, R.L. Artificial Neural Network control of thermoelectrically-cooled microfluidics using computer vision based on IR thermography. *Comput. Chem. Eng.* **2019**, *121*, 584–593. [[CrossRef](#)]
62. Quinn, D.; Thalheim, T.; Cichos, F. Microfluidics with feedback control and machine learning (Conference Presentation). In Proceedings of the Emerging Topics in Artificial Intelligence (ETAI) 2022, San Diego, CA, USA, 21–25 August 2022; SPIE: Bellingham, WA, USA: 2022; Volume PC12204, p. PC12204S. [[CrossRef](#)]
63. Lewis, C.; Erikson, J.W.; Sanchez, D.A.; McClure, C.E.; Nordin, G.P.; Munro, T.R.; Colton, J.S. Use of Machine Learning with Temporal Photoluminescence Signals from CdTe Quantum Dots for Temperature Measurement in Microfluidic Devices. *ACS Appl. Nano Mater.* **2020**, *3*, 4045–4053. [[CrossRef](#)] [[PubMed](#)]
64. Raymond, S.J.; Collins, D.J.; O'Rourke, R.; Tayebi, M.; Ai, Y.; Williams, J. A deep learning approach for designed diffraction-based acoustic patterning in microchannels. *Sci. Rep.* **2020**, *10*, 8745. [[CrossRef](#)] [[PubMed](#)]
65. Tang, Y.; Duan, F.; Zhou, A.; Kaniithamniyom, P.; Luo, S.; Hu, X.; Jiang, X.; Vasoo, S.; Zhang, X.; Zhang, Y. Image-based real-time feedback control of magnetic digital microfluidics by artificial intelligence-empowered rapid object detector for automated in vitro diagnostics. *Bioeng. Transl. Med.* **2022**, *e10428*. [[CrossRef](#)]
66. Zhang, S.; Wang, Y.; Onck, P.; den Toonder, J. A concise review of microfluidic particle manipulation methods. *Microfluid. Nanofluidics* **2020**, *24*, 24. [[CrossRef](#)]
67. Fang, W.Z.; Xiong, T.; Pak, O.S.; Zhu, L. Data-Driven Intelligent Manipulation of Particles in Microfluidics. *Adv. Sci.* **2022**, *10*, 2205382. [[CrossRef](#)]
68. Bazaz, S.R.; Mashhadian, A.; Ehsani, A.; Saha, S.C.; Krüger, T.; Warkiani, M.E. Computational inertial microfluidics: A review. *Lab Chip* **2020**, *20*, 1023–1048. [[CrossRef](#)] [[PubMed](#)]
69. Del Giudice, F. A Review of Microfluidic Devices for Rheological Characterisation. *Micromachines* **2022**, *13*, 167. [[CrossRef](#)]
70. Su, J.; Chen, X.; Zhu, Y.; Hu, G. Machine learning assisted fast prediction of inertial lift in microchannels. *Lab Chip* **2021**, *21*, 2544–2556. [[CrossRef](#)] [[PubMed](#)]

71. Hamdi, E.; Dezhkam, R.; Shamloo, A.; Mashhadian, A. microAI: A machine learning tool for fast calculation of lift coefficients in microchannels. *arXiv* **2022**. [[CrossRef](#)]
72. Zhang, Y.; Zhou, A.; Chen, S.; Lum, G.Z.; Zhang, X. A perspective on magnetic microfluidics: Towards an intelligent future. *Biomicrofluidics* **2022**, *16*, 011301. [[CrossRef](#)]
73. Koh, J.B.Y.; Shen, X.; Marcos. Supervised Learning to Predict Sperm Sorting by Magnetophoresis. *Magnetochemistry* **2018**, *4*, 31. [[CrossRef](#)]
74. Ciriza, D.B.; Magazzù, A.; Callegari, A.; Iati, M.A.; Volpe, G.; Maragò, O.M. Machine learning to enhance the calculation of optical forces in the geometrical optics approximation. In Proceedings of the Biophotonics Congress 2021, Washington, DC, USA, 12–16 April 2021; Optica Publishing Group, Washington, DC, USA, 2021; p. AF2D.3. [[CrossRef](#)]
75. Zhao, J.; Hou, H.; Huang, Q.Y.; Zhong, X.G.; Zheng, P.S. Design of Optical Tweezers Manipulation Control System Based on Novel Self-Organizing Fuzzy Cerebellar Model Neural Network. *Appl. Sci.* **2022**, *12*, 9655. [[CrossRef](#)]
76. Harshbarger, C.L.; Gerlt, M.S.; Ghadamian, J.A.; Bernardoni, D.C.; Snedeker, J.G.; Dual, J. Optical feedback control loop for the precise and robust acoustic focusing of cells, micro- and nanoparticles. *Lab Chip* **2022**, *22*, 2810–2819. [[CrossRef](#)]
77. Yiannacou, K.; Sariola, V. Controlled Manipulation and Active Sorting of Particles Inside Microfluidic Chips Using Bulk Acoustic Waves and Machine Learning. *Langmuir* **2021**, *37*, 4192–4199. [[CrossRef](#)]
78. Yiannacou, K.; Sharma, V.; Sariola, V. Programmable Droplet Microfluidics Based on Machine Learning and Acoustic Manipulation. *Langmuir* **2022**, *38*, 11557–11564. [[CrossRef](#)]
79. Teh, S.Y.; Lin, R.; Hung, L.H.; Lee, A.P. Droplet microfluidics. *Lab Chip* **2008**, *8*, 198–220. [[CrossRef](#)]
80. Pouyanfar, N.; Harofte, S.Z.; Soltani, M.; Siavashy, S.; Asadian, E.; Ghorbani-Bidkorbeh, F.; Keçili, R.; Hussain, C.M. Artificial intelligence-based microfluidic platforms for the sensitive detection of environmental pollutants: Recent advances and prospects. *Trends Environ. Anal. Chem.* **2022**, *34*, e00160. [[CrossRef](#)]
81. Mahdi, Y.; Daoud, K. Microdroplet size prediction in microfluidic systems via artificial neural network modeling for water-in-oil emulsion formulation. *J. Dispers. Sci. Technol.* **2017**, *38*, 1501–1508. [[CrossRef](#)]
82. Crowson, M.G.; Moukheiber, D.; Arévalo, A.R.; Lam, B.D.; Mantena, S.; Rana, A.; Goss, D.; Bates, D.W.; Celi, L.A. A systematic review of federated learning applications for biomedical data. *PLoS Digit. Health* **2022**, *1*, e0000033. [[CrossRef](#)] [[PubMed](#)]
83. Siemann, A.E.; Shaulsky, E.; Beveridge, M.; Buonassisi, T.; Hashmi, S.M.; Drori, I. A Machine Learning and Computer Vision Approach to Rapidly Optimize Multiscale Droplet Generation. *ACS Appl. Mater. Interfaces* **2022**, *14*, 4668–4679. [[CrossRef](#)]
84. Khor, J.W.; Jean, N.; Luxenberg, E.S.; Ermon, S.; Tang, S.K.Y. Using machine learning to discover shape descriptors for predicting emulsion stability in a microfluidic channel. *Soft Matter* **2019**, *15*, 1361–1372. [[CrossRef](#)]
85. Chagot, L.; Quilodrán-Casas, C.; Kalli, M.; Kovalchuk, N.M.; Simmons, M.J.H.; Matar, O.K.; Arcucci, R.; Angeli, P. Surfactant-laden droplet size prediction in a flow-focusing microchannel: A data-driven approach. *Lab Chip* **2022**, *22*, 3848–3859. [[CrossRef](#)]
86. Gardner, K.; Uddin, M.M.; Tran, L.; Pham, T.; Vanapalli, S.; Li, W. Deep learning detector for high precision monitoring of cell encapsulation statistics in microfluidic droplets. *Lab Chip* **2022**, *22*, 4067–4080. [[CrossRef](#)]
87. Rutkowski, G.P.; Azizov, I.; Unmann, E.; Dudek, M.; Grimes, B.A. Microfluidic droplet detection via region-based and single-pass convolutional neural networks with comparison to conventional image analysis methodologies. *Mach. Learn. Appl.* **2022**, *7*, 10022. [[CrossRef](#)]
88. Vaithianathan, M.; Safa, N.; Melvin, A.T. FluoroCellTrack: An algorithm for automated analysis of high-throughput droplet microfluidic data. *PLoS ONE* **2019**, *14*, e0215337. [[CrossRef](#)]
89. Durve, M.; Tiribocchi, A.; Bonaccorso, F.; Montessori, A.; Lauricella, M.; Bogdan, M.; Guzowski, J.; Succi, S. DropTrack – automatic droplet tracking using deep learning for microfluidic applications. *Phys. Fluids* **2022**, *34*, 082003. [[CrossRef](#)]
90. Zhuang, Y.; Cheng, S.; Kovalchuk, N.; Simmons, M.; Matar, O.K.; Guo, Y.K.; Arcucci, R. Ensemble latent assimilation with deep learning surrogate model: application to drop interaction in a microfluidics device. *Lab Chip* **2022**, *22*, 3187–3202. [[CrossRef](#)]
91. Hadikhani, P.; Borhani, N.; Hashemi, S.M.; Psaltis, D. Learning from droplet flows in microfluidic channels using deep neural networks. *Sci. Rep.* **2019**, *9*, 8114. [[CrossRef](#)]
92. Arjun, A.; Ajith, R.R.; Kumar Ranjith, S. Mixing characterization of binary-coalesced droplets in microchannels using deep neural network. *Biomicrofluidics* **2020**, *14*, 034111. [[CrossRef](#)]
93. Roy, P.; House, M.L.; Dutcher, C.S. A Microfluidic Device for Automated High Throughput Detection of Ice Nucleation of Snomax®. *Micromachines* **2021**, *12*, 296. [[CrossRef](#)]
94. Liang, T.C.; Zhong, Z.; Bigdely, Y.; Ho, T.Y.; Chakrabarty, K.; Fair, R. Adaptive Droplet Routing in Digital Microfluidic Biochips Using Deep Reinforcement Learning. In Proceedings of the 37th International Conference on Machine Learning, Virtual, 13–18 July 2020; PMLR: Cambridge, MA, USA, 2020; pp. 6050–6060.
95. Jiang, C.; Yang, R.Q.; Yuan, B. An evolutionary algorithm with indirect representation for droplet routing in digital microfluidic biochips. *Eng. Appl. Artif. Intell.* **2022**, *115*, 105305. [[CrossRef](#)]
96. Chu, A.; Nguyen, D.; Talathi, S.S.; Wilson, A.C.; Ye, C.; Smith, W.L.; Kaplan, A.D.; Duoss, E.B.; Stolaroff, J.K.; Giera, B. Automated detection and sorting of microencapsulation via machine learning. *Lab Chip* **2019**, *19*, 1808–1817. [[CrossRef](#)] [[PubMed](#)]
97. Anagnostidis, V.; Sherlock, B.; Metz, J.; Mair, P.; Hollfelder, F.; Gielen, F. Deep learning guided image-based droplet sorting for on-demand selection and analysis of single cells and 3D cell cultures. *Lab Chip* **2020**, *20*, 889–900. [[CrossRef](#)] [[PubMed](#)]
98. Howell, L.; Anagnostidis, V.; Gielen, F. Multi-Object Detector YOLOv4-Tiny Enables High-Throughput Combinatorial and Spatially-Resolved Sorting of Cells in Microdroplets. *Adv. Mater. Technol.* **2022**, *7*, 2101053. [[CrossRef](#)]

99. Liu, L.; Bi, M.; Wang, Y.; Liu, J.; Jiang, X.; Xu, Z.; Zhang, X. Artificial intelligence-powered microfluidics for nanomedicine and materials synthesis. *Nanoscale* **2021**, *13*, 19352–19366. [[CrossRef](#)]
100. Reizman, B.J.; Jensen, K.F. Feedback in Flow for Accelerated Reaction Development. *Acc. Chem. Res.* **2016**, *49*, 1786–1796. [[CrossRef](#)]
101. Granda, J.M.; Donina, L.; Dragone, V.; Long, D.L.; Cronin, L. Controlling an organic synthesis robot with machine learning to search for new reactivity. *Nature* **2018**, *559*, 377–381. [[CrossRef](#)] [[PubMed](#)]
102. Zhong, J.; Riordon, J.; Wu, T.C.; Edwards, H.; Wheeler, A.R.; Pardee, K.; Aspuru-Guzik, A.; Sinton, D. When robotics met fluidics. *Lab Chip* **2020**, *20*, 709–716. [[CrossRef](#)]
103. McMullen, J.P.; Jensen, K.F. An Automated Microfluidic System for Online Optimization in Chemical Synthesis. *Org. Process Res. Dev.* **2010**, *14*, 1169–1176. [[CrossRef](#)]
104. McMullen, J.P.; Stone, M.T.; Buchwald, S.L.; Jensen, K.F. An Integrated Microreactor System for Self-Optimization of a Heck Reaction: From Micro- to Mesoscale Flow Systems. *Angew. Chem. Int. Ed.* **2010**, *49*, 7076–7080. [[CrossRef](#)]
105. Rizkin, B.A.; Shkolnik, A.S.; Ferraro, N.J.; Hartman, R.L. Combining automated microfluidic experimentation with machine learning for efficient polymerization design. *Nat. Mach. Intell.* **2020**, *2*, 200–209. [[CrossRef](#)]
106. Chen, X.; Lv, H. Intelligent control of nanoparticle synthesis on microfluidic chips with machine learning. *NPG Asia Mater.* **2022**, *14*, 1–20. [[CrossRef](#)]
107. Krishnadasan, S.; Brown, R.J.C.; deMello, A.J.; deMello, J.C. Intelligent routes to the controlled synthesis of nanoparticles. *Lab Chip* **2007**, *7*, 1434–1441. [[CrossRef](#)] [[PubMed](#)]
108. Orimoto, Y.; Watanabe, K.; Yamashita, K.; Uehara, M.; Nakamura, H.; Furuya, T.; Maeda, H. Application of Artificial Neural Networks to Rapid Data Analysis in Combinatorial Nanoparticle Syntheses. *J. Phys. Chem. C* **2012**, *116*, 17885–17896. [[CrossRef](#)]
109. Ahrberg, C.D.; Wook Choi, J.; Geun Chung, B. Automated droplet reactor for the synthesis of iron oxide/gold core-shell nanoparticles. *Sci. Rep.* **2020**, *10*, 1737. [[CrossRef](#)]
110. Mekki-Berrada, F.; Ren, Z.; Huang, T.; Wong, W.K.; Zheng, F.; Xie, J.; Tian, I.P.S.; Jayavelu, S.; Mahfoud, Z.; Bash, D.; et al. Two-step machine learning enables optimized nanoparticle synthesis. *Npj Comput. Mater.* **2021**, *7*, 1–10. [[CrossRef](#)]
111. Tao, H.; Wu, T.; Kheiri, S.; Aldeghi, M.; Aspuru-Guzik, A.; Kumacheva, E. Self-Driving Platform for Metal Nanoparticle Synthesis: Combining Microfluidics and Machine Learning. *Adv. Funct. Mater.* **2021**, *31*, 2106725. [[CrossRef](#)]
112. Volk, A.A.; Epps, R.W.; Abolhasani, M. Accelerated Development of Colloidal Nanomaterials Enabled by Modular Microfluidic Reactors: Toward Autonomous Robotic Experimentation. *Adv. Mater.* **2021**, *33*, 2004495. [[CrossRef](#)]
113. Wahl, C.B.; Aykol, M.; Swisher, J.H.; Montoya, J.H.; Suram, S.K.; Mirkin, C.A. Machine learning–accelerated design and synthesis of polyelemental heterostructures. *Sci. Adv.* **2021**, *7*, eabj5505. [[CrossRef](#)]
114. Wang, S.; Shen, Z.; Shen, Z.; Dong, Y.; Li, Y.; Cao, Y.; Zhang, Y.; Guo, S.; Shuai, J.; Yang, Y.; et al. Machine-learning micropattern manufacturing. *Nano Today* **2021**, *38*, 101152. [[CrossRef](#)]
115. Ali, H.S.M.; Blagden, N.; York, P.; Amani, A.; Brook, T. Artificial neural networks modelling the prednisolone nanoprecipitation in microfluidic reactors. *Eur. J. Pharm. Sci.* **2009**, *37*, 514–522. [[CrossRef](#)]
116. Kirmani, A.R.; Luther, J.M.; Abolhasani, M.; Amassian, A. Colloidal Quantum Dot Photovoltaics: Current Progress and Path to Gigawatt Scale Enabled by Smart Manufacturing. *ACS Energy Lett.* **2020**, *5*, 3069–3100. [[CrossRef](#)]
117. Chen, G.; Zhu, X.; Xing, C.; Wang, Y.; Xu, X.; Bao, J.; Huang, J.; Zhao, Y.; Wang, X.; Zhou, X.; et al. Machine Learning-Assisted Microfluidic Synthesis of Perovskite Quantum Dots. *Adv. Photonics Res.* **2022**, *4*, 2200230. [[CrossRef](#)]
118. Rebollo, R.; Oyoun, F.; Corvis, Y.; El-Hammadi, M.M.; Saubamea, B.; Andrieux, K.; Mignet, N.; Alhareth, K. Microfluidic Manufacturing of Liposomes: Development and Optimization by Design of Experiment and Machine Learning. *ACS Appl. Mater. Interfaces* **2022**, *14*, 39736–39745. [[CrossRef](#)] [[PubMed](#)]
119. Damiati, S.A.; Rossi, D.; Joensson, H.N.; Damiati, S. Artificial intelligence application for rapid fabrication of size-tunable PLGA microparticles in microfluidics. *Sci. Rep.* **2020**, *10*, 19517. [[CrossRef](#)] [[PubMed](#)]
120. Damiati, S.A.; Damiati, S. Microfluidic Synthesis of Indomethacin-Loaded PLGA Microparticles Optimized by Machine Learning. *Front. Mol. Biosci.* **2021**, *8*, 595. [[CrossRef](#)] [[PubMed](#)]
121. Grisoni, F.; Huisman, B.J.H.; Button, A.L.; Moret, M.; Atz, K.; Merk, D.; Schneider, G. Combining generative artificial intelligence and on-chip synthesis for de novo drug design. *Sci. Adv.* **2021**, *7*, eabg3338. [[CrossRef](#)] [[PubMed](#)]
122. Schneider, G. Automating drug discovery. *Nat. Rev. Drug Discov.* **2018**, *17*, 97–113. [[CrossRef](#)] [[PubMed](#)]
123. Liu, Y.; Sun, L.; Zhang, H.; Shang, L.; Zhao, Y. Microfluidics for Drug Development: From Synthesis to Evaluation. *Chem. Rev.* **2021**, *121*, 7468–7529. [[CrossRef](#)]
124. Popova, M.; Isayev, O.; Tropsha, A. Deep reinforcement learning for de novo drug design. *Sci. Adv.* **2018**, *4*, eaap7885. [[CrossRef](#)]
125. Bannigan, P.; Bao, Z.; Hickman, R.J.; Aldeghi, M.; Häse, F.; Aspuru-Guzik, A.; Allen, C. Machine learning models to accelerate the design of polymeric long-acting injectables. *Nat. Commun.* **2023**, *14*, 35. [[CrossRef](#)]
126. Mejía-Salazar, J.R.; Rodrigues Cruz, K.; Materón Vásques, E.M.; Novais de Oliveira, O., Jr. Microfluidic Point-of-Care Devices: New Trends and Future Prospects for eHealth Diagnostics. *Sensors* **2020**, *20*, 1951. [[CrossRef](#)]
127. Zare Harofte, S.; Soltani, M.; Siavashy, S.; Raahemifar, K. Recent Advances of Utilizing Artificial Intelligence in Lab on a Chip for Diagnosis and Treatment. *Small* **2022**, *18*, 2203169. [[CrossRef](#)]
128. Romao, V.C.; Martins, S.A.M.; Germano, J.; Cardoso, F.A.; Cardoso, S.; Freitas, P.P. Lab-on-Chip Devices: Gaining Ground Losing Size. *ACS Nano* **2017**, *11*, 10659–10664. [[CrossRef](#)]

129. Dabbagh, S.R.; Rabbi, F.; Doğan, Z.; Yetisen, A.K.; Tasoglu, S. Machine learning-enabled multiplexed microfluidic sensors. *Biomicrofluidics* **2020**, *14*, 061506. [[CrossRef](#)]
130. Lee, W.; Gonzalez, A.; Arguelles, P.; Guevara, R.; Gonzalez-Guerrero, M.J.; Gomez, F.A. Thread/paper- and paper-based microfluidic devices for glucose assays employing artificial neural networks. *Electrophoresis* **2018**, *39*, 1443–1451. [[CrossRef](#)] [[PubMed](#)]
131. Mercan, Ö.B.; Kılıç, V.; Şen, M. Machine learning-based colorimetric determination of glucose in artificial saliva with different reagents using a smartphone coupled μPAD. *Sens. Actuators Chem.* **2021**, *329*, 129037. [[CrossRef](#)]
132. Muñoz, H.E.; Riche, C.T.; Kong, J.E.; van Zee, M.; Garner, O.B.; Ozcan, A.; Di Carlo, D. Fractal LAMP: Label-Free Analysis of Fractal Precipitate for Digital Loop-Mediated Isothermal Nucleic Acid Amplification. *ACS Sens.* **2020**, *5*, 385–394. [[CrossRef](#)] [[PubMed](#)]
133. Alvarez, M.; Rahmani, E.; Jew, B.; Garske, K.M.; Miao, Z.; Benhammou, J.N.; Ye, C.J.; Pisegna, J.R.; Pietiläinen, K.H.; Halperin, E.; et al. Enhancing droplet-based single-nucleus RNA-seq resolution using the semi-supervised machine learning classifier DIEM. *Sci. Rep.* **2020**, *10*, 11019. [[CrossRef](#)]
134. Lee, T.H.; Kwon, H.B.; Song, W.Y.; Lee, S.S.; Kim, Y.J. Microfluidic ultrafine particle dosimeter using an electrical detection method with a machine-learning-aided algorithm for real-time monitoring of particle density and size distribution. *Lab Chip* **2021**, *21*, 1503–1516. [[CrossRef](#)] [[PubMed](#)]
135. Alapan, Y.; Kim, C.; Adhikari, A.; Gray, K.E.; Gurkan-Cavusoglu, E.; Little, J.A.; Gurkan, U.A. Sickle cell disease biochip: A functional red blood cell adhesion assay for monitoring sickle cell disease. *Transl. Res.* **2016**, *173*, 74–91.e8. [[CrossRef](#)]
136. Praljak, N.; Iram, S.; Goreke, U.; Singh, G.; Hill, A.; Gurkan, U.A.; Hinczewski, M. Integrating deep learning with microfluidics for biophysical classification of sickle red blood cells adhered to laminin. *PLoS Comput. Biol.* **2021**, *17*, e1008946. [[CrossRef](#)]
137. Lamoureux, E.S.; Islamzada, E.; Wiens, M.V.J.; Matthews, K.; Duffy, S.P.; Ma, H. Assessing red blood cell deformability from microscopy images using deep learning. *Lab Chip* **2021**, *22*, 26–39. [[CrossRef](#)]
138. Rizzuto, V.; Mencattini, A.; Álvarez González, B.; Di Giuseppe, D.; Martinelli, E.; Beneitez-Pastor, D.; Mañú-Pereira, M.d.M.; Lopez-Martinez, M.J.; Samitier, J. Combining microfluidics with machine learning algorithms for RBC classification in rare hereditary hemolytic anemia. *Sci. Rep.* **2021**, *11*, 13553. [[CrossRef](#)]
139. Ellett, F.; Jorgensen, J.; Marand, A.L.; Liu, Y.M.; Martinez, M.M.; Sein, V.; Butler, K.L.; Lee, J.; Irimia, D. Diagnosis of sepsis from a drop of blood by measurement of spontaneous neutrophil motility in a microfluidic assay. *Nat. Biomed. Eng.* **2018**, *2*, 207–214. [[CrossRef](#)]
140. Kalmady, K.S.; Kamath, A.S.; Gopakumar, G.; Subrahmanyam, G.R.K.S.; Gorthi, S.S. Improved Transfer Learning through Shallow Network Embedding for Classification of Leukemia Cells. In Proceedings of the 2017 Ninth International Conference on Advances in Pattern Recognition (ICAPR), Bangalore, India, 27–30 December 2017; pp. 1–6. [[CrossRef](#)]
141. Gopakumar, G.; Hari Babu, K.; Mishra, D.; Gorthi, S.S.; Sai Subrahmanyam, G.R.K. Cytopathological image analysis using deep-learning networks in microfluidic microscopy. *J. Opt. Soc. Am. A Opt. Image Sci. Vis.* **2017**, *34*, 111–121. [[CrossRef](#)] [[PubMed](#)]
142. Manak, M.S.; Varsanik, J.S.; Hogan, B.J.; Whitfield, M.J.; Su, W.R.; Joshi, N.; Steinke, N.; Min, A.; Berger, D.; Saphirstein, R.J.; et al. Live-cell phenotypic-biomarker microfluidic assay for the risk stratification of cancer patients via machine learning. *Nat. Biomed. Eng.* **2018**, *2*, 761–772. [[CrossRef](#)] [[PubMed](#)]
143. Soldati, G.; Del Ben, F.; Brisotto, G.; Biscontin, E.; Bulfoni, M.; Piruska, A.; Steffan, A.; Turetta, M.; Della Mea, V. Microfluidic droplets content classification and analysis through convolutional neural networks in a liquid biopsy workflow. *Am. J. Transl. Res.* **2018**, *10*, 4004–4016. [[PubMed](#)]
144. Hashemzadeh, H.; Shojaeilangari, S.; Allahverdi, A.; Rothbauer, M.; Ertl, P.; Naderi-Manesh, H. A combined microfluidic deep learning approach for lung cancer cell high throughput screening toward automatic cancer screening applications. *Sci. Rep.* **2021**, *11*, 9804. [[CrossRef](#)]
145. Ayensa-Jiménez, J.; Doweidar, M.H.; Sanz-Herrera, J.A.; Doblare, M. Understanding glioblastoma invasion using physically-guided neural networks with internal variables. *PLoS Comput. Biol.* **2022**, *18*, e1010019. [[CrossRef](#)]
146. Ni, W.; Hu, B.; Zheng, C.; Tong, Y.; Wang, L.; Li, Q.Q.; Tong, X.; Han, Y. Automated analysis of acute myeloid leukemia minimal residual disease using a support vector machine. *Oncotarget* **2016**, *7*, 71915–71921. [[CrossRef](#)]
147. Turan, B.; Masuda, T.; Lei, W.; Noor, A.M.; Horio, K.; Saito, T.I.; Miyata, Y.; Arai, F. A pillar-based microfluidic chip for T-cells and B-cells isolation and detection with machine learning algorithm. *ROBOMECH J.* **2018**, *5*, 27. [[CrossRef](#)]
148. McRae, M.P.; Simmons, G.W.; Wong, J.; Shadfan, B.; Gopalkrishnan, S.; Christodoulides, N.; McDevitt, J.T. Programmable bio-nano-chip system: A flexible point-of-care platform for bioscience and clinical measurements. *Lab Chip* **2015**, *15*, 4020–4031. [[CrossRef](#)]
149. Christodoulides, N.; De La Garza, R.; Simmons, G.W.; McRae, M.P.; Wong, J.; Newton, T.F.; Smith, R.; Mahoney III, J.J.; Hohenstein, J.; Gomez, S.; et al. Application of programmable bio-nano-chip system for the quantitative detection of drugs of abuse in oral fluids. *Drug Alcohol Depend.* **2015**, *153*, 306–313. [[CrossRef](#)]
150. McRae, M.P.; Simmons, G.; Wong, J.; McDevitt, J.T. Programmable Bio-nanochip Platform: A Point-of-Care Biosensor System with the Capacity To Learn. *Acc. Chem. Res.* **2016**, *49*, 1359–1368. [[CrossRef](#)] [[PubMed](#)]
151. Song, Y.; Zhao, J.; Cai, T.; Stephens, A.; Su, S.H.; Sandford, E.; Flora, C.; Singer, B.H.; Ghosh, M.; Choi, S.W.; et al. Machine learning-based cytokine microarray digital immunoassay analysis. *Biosens. Bioelectron.* **2021**, *180*, 113088. [[CrossRef](#)] [[PubMed](#)]

152. Ross, G.M.S.; Filippini, D.; Nielsen, M.W.F.; Salentijn, G.I. Unraveling the Hook Effect: A Comprehensive Study of High Antigen Concentration Effects in Sandwich Lateral Flow Immunoassays. *Anal. Chem.* **2020**, *92*, 15587–15595. [CrossRef] [PubMed]
153. Banaei, N.; Moshfegh, J.; Mohseni-Kabir, A.; Houghton, J.M.; Sun, Y.; Kim, B. Machine learning algorithms enhance the specificity of cancer biomarker detection using SERS-based immunoassays in microfluidic chips. *RSC Adv.* **2019**, *9*, 1859–1868. [CrossRef] [PubMed]
154. Luo, Y.; Joung, H.A.; Esparza, S.; Rao, J.; Garner, O.; Ozcan, A. Quantitative particle agglutination assay for point-of-care testing using mobile holographic imaging and deep learning. *Lab Chip* **2021**, *21*, 3550–3558. [CrossRef] [PubMed]
155. Chen, H.; Kim, S.; Hardie, J.M.; Thirumalaraju, P.; Gharpure, S.; Rostamian, S.; Udayakumar, S.; Lei, Q.; Cho, G.; Kanakasabapathy, M.K.; et al. Deep learning-assisted sensitive detection of fentanyl using a bubbling-microchip. *Lab Chip* **2022**, *22*, 4531–4540. [CrossRef] [PubMed]
156. Dhama, K.; Khan, S.; Tiwari, R.; Sircar, S.; Bhat, S.; Malik, Y.S.; Singh, K.P.; Chaicumpa, W.; Bonilla-Aldana, D.K.; Rodriguez-Morales, A.J. Coronavirus Disease 2019–COVID-19. *Clin. Microbiol. Rev.* **2020**, *33*, e00028-20. [CrossRef]
157. Wiersinga, W.J.; Rhodes, A.; Cheng, A.C.; Peacock, S.J.; Prescott, H.C. Pathophysiology, Transmission, Diagnosis, and Treatment of Coronavirus Disease 2019 (COVID-19): A Review. *JAMA* **2020**, *324*, 782–793. [CrossRef]
158. Funari, R.; Chu, K.Y.; Shen, A.Q. Detection of antibodies against SARS-CoV-2 spike protein by gold nanospikes in an opto-microfluidic chip. *Biosens. Bioelectron.* **2020**, *169*, 112578. [CrossRef]
159. Jamiruddin, M.R.; Meghla, B.A.; Islam, D.Z.; Tisha, T.A.; Khandker, S.S.; Khondoker, M.U.; Haq, M.A.; Adnan, N.; Haque, M. Microfluidics Technology in SARS-CoV-2 Diagnosis and Beyond: A Systematic Review. *Life* **2022**, *12*, 649. [CrossRef]
160. Li, Q.; Zhou, X.; Wang, Q.; Liu, W.; Chen, C. Microfluidics for COVID-19: From Current Work to Future Perspective. *Biosensors* **2023**, *13*, 163. [CrossRef]
161. Bhuiyan, N.H.; Hong, J.H.; Uddin, M.J.; Shim, J.S. Artificial Intelligence-Controlled Microfluidic Device for Fluid Automation and Bubble Removal of Immunoassay Operated by a Smartphone. *Anal. Chem.* **2022**, *94*, 3872–3880. [CrossRef] [PubMed]
162. Bhuiyan, N.H.; Uddin, M.J.; Lee, J.; Hong, J.H.; Shim, J.S. An Internet-of-Disease System for COVID-19 Testing Using Saliva by an AI-Controlled Microfluidic ELISA Device. *Adv. Mater. Technol.* **2022**, *7*, 2101690. [CrossRef] [PubMed]
163. Xia, T.; Fu, Y.Q.; Jin, N.; Chazot, P.; Angelov, P.; Jiang, R. AI-enabled Microscopic Blood Analysis for Microfluidic COVID-19 Hematology. In Proceedings of the 2020 5th International Conference on Computational Intelligence and Applications (ICCIA), Beijing, China, 19–21 June 2020; pp. 98–102. [CrossRef]
164. Gao, Z.; Song, Y.; Hsiao, T.Y.; He, J.; Wang, C.; Shen, J.; MacLachlan, A.; Dai, S.; Singer, B.H.; Kurabayashi, K.; et al. Machine-Learning-Assisted Microfluidic Nanoplasmonic Digital Immunoassay for Cytokine Storm Profiling in COVID-19 Patients. *ACS Nano* **2021**, *15*, 18023–18036. [CrossRef] [PubMed]
165. Potter, C.J.; Hu, Y.; Xiong, Z.; Wang, J.; McLeod, E. Point-of-care SARS-CoV-2 sensing using lens-free imaging and a deep learning-assisted quantitative agglutination assay. *Lab Chip* **2022**, *22*, 3744–3754. [CrossRef]
166. Wang, B.; Li, Y.; Zhou, M.; Han, Y.; Zhang, M.; Gao, Z.; Liu, Z.; Chen, P.; Du, W.; Zhang, X.; et al. Smartphone-based platforms implementing microfluidic detection with image-based artificial intelligence. *Nat. Commun.* **2023**, *14*, 1341. [CrossRef]
167. Kumar, A.; Parihar, A.; Panda, U.; Parihar, D.S. Microfluidics-Based Point-of-Care Testing (POCT) Devices in Dealing with Waves of COVID-19 Pandemic: The Emerging Solution. *ACS Appl. Bio Mater.* **2022**, *5*, 2046–2068. [CrossRef]
168. Ramezankhani, R.; Solhi, R.; Chai, Y.C.; Vosough, M.; Verfaillie, C. Organoid and microfluidics-based platforms for drug screening in COVID-19. *Drug Discov. Today* **2022**, *27*, 1062–1076. [CrossRef]
169. Chiu, H.Y.R.; Hwang, C.K.; Chen, S.Y.; Shih, F.Y.; Han, H.C.; King, C.C.; Gilbert, J.R.; Fang, C.C.; Oyang, Y.J. Machine learning for emerging infectious disease field responses. *Sci. Rep.* **2022**, *12*, 328. [CrossRef]
170. Tran, N.K.; Albahra, S.; May, L.; Waldman, S.; Crabtree, S.; Bainbridge, S.; Rashidi, H. Evolving Applications of Artificial Intelligence and Machine Learning in Infectious Diseases Testing. *Clin. Chem.* **2022**, *68*, 125–133. [CrossRef]
171. Zhang, Z.; Chen, L.; Wang, Y.; Zhang, T.; Chen, Y.C.; Yoon, E. Label-Free Estimation of Therapeutic Efficacy on 3D Cancer Spheres Using Convolutional Neural Network Image Analysis. *Anal. Chem.* **2019**, *91*, 14093–14100. [CrossRef] [PubMed]
172. Lin, S.; Hu, S.; Song, W.; Gu, M.; Liu, J.; Song, J.; Liu, Z.; Li, Z.; Huang, K.; Wu, Y.; et al. An ultralight, flexible, and biocompatible all-fiber motion sensor for artificial intelligence wearable electronics. *Npj Flex. Electron.* **2022**, *6*, 1–8. [CrossRef]
173. Kobayashi, H.; Lei, C.; Wu, Y.; Mao, A.; Jiang, Y.; Guo, B.; Ozeki, Y.; Goda, K. Label-free detection of cellular drug responses by high-throughput bright-field imaging and machine learning. *Sci. Rep.* **2017**, *7*, 12454. [CrossRef]
174. Kobayashi, H.; Lei, C.; Wu, Y.; Huang, C.J.; Yasumoto, A.; Jona, M.; Li, W.; Wu, Y.; Yalikun, Y.; Jiang, Y.; et al. Intelligent whole-blood imaging flow cytometry for simple, rapid, and cost-effective drug-susceptibility testing of leukemia. *Lab Chip* **2019**, *19*, 2688–2698. [CrossRef] [PubMed]
175. Zhou, Y.; Yasumoto, A.; Lei, C.; Huang, C.J.; Kobayashi, H.; Wu, Y.; Yan, S.; Sun, C.W.; Yatomi, Y.; Goda, K. Intelligent classification of platelet aggregates by agonist type. *eLife* **2020**, *9*, e52938. [CrossRef] [PubMed]
176. Lv, J.; Deng, S.; Zhang, L. A review of artificial intelligence applications for antimicrobial resistance. *Biosaf. Health* **2021**, *3*, 22–31. [CrossRef]
177. Poweleit, E.A.; Vinks, A.A.; Mizuno, T. Artificial Intelligence and Machine Learning Approaches to Facilitate Therapeutic Drug Management and Model-Informed Precision Dosing. *Ther. Drug Monit.* **2022**, *45*, 143–150. [CrossRef]
178. Yu, H.; Jing, W.; Iriya, R.; Yang, Y.; Syal, K.; Mo, M.; Gris, T.E.; Haydel, S.E.; Wang, S.; Tao, N. Phenotypic Antimicrobial Susceptibility Testing with Deep Learning Video Microscopy. *Anal. Chem.* **2018**, *90*, 6314–6322. [CrossRef]

179. Kim, K.; Kim, S.; Jeon, J.S. Visual Estimation of Bacterial Growth Level in Microfluidic Culture Systems. *Sensors* **2018**, *18*, 447. [[CrossRef](#)]
180. Svensson, C.M.; Shvydkiv, O.; Dietrich, S.; Mahler, L.; Weber, T.; Choudhary, M.; Tovar, M.; Figge, M.T.; Roth, M. Coding of Experimental Conditions in Microfluidic Droplet Assays Using Colored Beads and Machine Learning Supported Image Analysis. *Small* **2019**, *15*, 1802384. [[CrossRef](#)]
181. Rauf, S.; Tashkandi, N.; de Oliveira Filho, J.I.; Oviedo-Osornio, C.I.; Danish, M.S.; Hong, P.Y.; Salama, K.N. Digital *E. coli* Counter: A Microfluidics and Computer Vision-Based DNAzyme Method for the Isolation and Specific Detection of *E. coli* from Water Samples. *Biosensors* **2022**, *12*, 34. [[CrossRef](#)] [[PubMed](#)]
182. Alves, V.M.; Auerbach, S.S.; Kleinstreuer, N.; Rooney, J.P.; Muratov, E.N.; Rusyn, I.; Tropsha, A.; Schmitt, C. Curated Data In—Trustworthy In Silico Models Out: The Impact of Data Quality on the Reliability of Artificial Intelligence Models as Alternatives to Animal Testing. *Altern. Lab. Anim.* **2021**, *49*, 73–82. [[CrossRef](#)] [[PubMed](#)]
183. Zhang, Y.; Tao, T.H. Skin-Friendly Electronics for Acquiring Human Physiological Signatures. *Adv. Mater.* **2019**, *31*, 1905767. [[CrossRef](#)]
184. Huang, J.D.; Wang, J.; Ramsey, E.; Leavey, G.; Chico, T.J.A.; Condell, J. Applying Artificial Intelligence to Wearable Sensor Data to Diagnose and Predict Cardiovascular Disease: A Review. *Sensors* **2022**, *22*, 8002. [[CrossRef](#)]
185. Rodríguez-Rodríguez, I.; Rodríguez, J.V.; Chatzigiannakis, I.; Zamora Izquierdo, M.A. On the Possibility of Predicting Glycaemia ‘On the Fly’ with Constrained IoT Devices in Type 1 Diabetes Mellitus Patients. *Sensors* **2019**, *19*, 4538. [[CrossRef](#)] [[PubMed](#)]
186. Sankhala, D.; Sardesai, A.U.; Pali, M.; Lin, K.C.; Jagannath, B.; Muthukumar, S.; Prasad, S. A machine learning-based on-demand sweat glucose reporting platform. *Sci. Rep.* **2022**, *12*, 2442. [[CrossRef](#)]
187. Han, S.; Kim, T.; Kim, D.; Park, Y.L.; Jo, S. Use of Deep Learning for Characterization of Microfluidic Soft Sensors. *IEEE Robot. Autom. Lett.* **2018**, *3*, 873–880. [[CrossRef](#)]
188. Kim, D.; Kim, M.; Kwon, J.; Park, Y.L.; Jo, S. Semi-Supervised Gait Generation with Two Microfluidic Soft Sensors. *IEEE Robot. Autom. Lett.* **2019**, *4*, 2501–2507. [[CrossRef](#)]
189. Wang, Y.; Shan, G.; Li, H.; Wang, L. A Wearable-Sensor System with AI Technology for Real-Time Biomechanical Feedback Training in Hammer Throw. *Sensors* **2023**, *23*, 425. [[CrossRef](#)]
190. Zhang, Y.; Hu, Y.; Jiang, N.; Yetisen, A.K. Wearable artificial intelligence biosensor networks. *Biosens. Bioelectron.* **2023**, *219*, 114825. [[CrossRef](#)]
191. Helmy, M.; Smith, D.; Selvarajoo, K. Systems biology approaches integrated with artificial intelligence for optimized metabolic engineering. *Metab. Eng. Commun.* **2020**, *11*, e00149. [[CrossRef](#)] [[PubMed](#)]
192. Riordon, J.; Sovilj, D.; Sanner, S.; Sinton, D.; Young, E.W.K. Deep Learning with Microfluidics for Biotechnology. *Trends Biotechnol.* **2019**, *37*, 310–324. [[CrossRef](#)]
193. Raji, H.; Tayyab, M.; Sui, J.; Mahmoodi, S.R.; Javanmard, M. Biosensors and machine learning for enhanced detection, stratification, and classification of cells: A review. *Biomed. Microdevices* **2022**, *24*, 26. [[CrossRef](#)]
194. Yang Yu, B.; Elbuken, C.; Ren, C.L.; Huissoon, J.P. Image processing and classification algorithm for yeast cell morphology in a microfluidic chip. *J. Biomed. Opt.* **2011**, *16*, 066008. [[CrossRef](#)]
195. Huang, X.; Guo, J.; Wang, X.; Yan, M.; Kang, Y.; Yu, H. A Contact-Imaging Based Microfluidic Cytometer with Machine-Learning for Single-Frame Super-Resolution Processing. *PLoS ONE* **2014**, *9*, e104539. [[CrossRef](#)] [[PubMed](#)]
196. Wang, N.; Liu, R.; Asmare, N.; Chu, C.H.; Sarioglu, A.F. Processing code-multiplexed Coulter signals via deep convolutional neural networks. *Lab Chip* **2019**, *19*, 3292–3304. [[CrossRef](#)] [[PubMed](#)]
197. Chen, J.; Zheng, Y.; Tan, Q.; Shojaei-Baghini, E.; Zhang, Y.L.; Li, J.; Prasad, P.; You, L.; Wu, X.Y.; Sun, Y. Classification of cell types using a microfluidic device for mechanical and electrical measurement on single cells. *Lab Chip* **2011**, *11*, 3174–3181. [[CrossRef](#)]
198. Heo, Y.J.; Lee, D.; Kang, J.; Lee, K.; Chung, W.K. Real-time Image Processing for Microscopy-based Label-free Imaging Flow Cytometry in a Microfluidic Chip. *Sci. Rep.* **2017**, *7*, 11651. [[CrossRef](#)]
199. Constantinou, I.; Jendrusch, M.; Aspert, T.; Görlitz, F.; Schulze, A.; Charvin, G.; Knop, M. Self-Learning Microfluidic Platform for Single-Cell Imaging and Classification in Flow. *Micromachines* **2019**, *10*, 311. [[CrossRef](#)]
200. Mikami, H.; Kawaguchi, M.; Huang, C.J.; Matsumura, H.; Sugimura, T.; Huang, K.; Lei, C.; Ueno, S.; Miura, T.; Ito, T.; et al. Virtual-freezing fluorescence imaging flow cytometry. *Nat. Commun.* **2020**, *11*, 1162. [[CrossRef](#)]
201. Huang, K.; Matsumura, H.; Zhao, Y.; Herbig, M.; Yuan, D.; Mineharu, Y.; Harmon, J.; Findinier, J.; Yamagishi, M.; Ohnuki, S.; et al. Deep imaging flow cytometry. *Lab Chip* **2022**, *22*, 876–889. [[CrossRef](#)]
202. Ahmad, A.; Sala, F.; Paiè, P.; Candeo, A.; D’Annunzio, S.; Zippo, A.; Frindel, C.; Osellame, R.; Bragheri, F.; Bassi, A.; et al. On the robustness of machine learning algorithms toward microfluidic distortions for cell classification via on-chip fluorescence microscopy. *Lab Chip* **2022**, *22*, 3453–3463. [[CrossRef](#)] [[PubMed](#)]
203. Rossi, D.; Dannhauser, D.; Telesco, M.; Netti, P.A.; Causa, F. CD4+ versus CD8+ T-lymphocyte identification in an integrated microfluidic chip using light scattering and machine learning. *Lab Chip* **2019**, *19*, 3888–3898. [[CrossRef](#)] [[PubMed](#)]
204. Wang, Y.; Wang, J.; Meng, J.; Ding, G.; Shi, Z.; Wang, R.; Zhang, X. Detection of non-small cell lung cancer cells based on microfluidic polarization microscopic image analysis. *Electrophoresis* **2019**, *40*, 1202–1211. [[CrossRef](#)]
205. Singh, D.K.; Ahrens, C.C.; Li, W.; Vanapalli, S.A. Label-free, high-throughput holographic screening and enumeration of tumor cells in blood. *Lab Chip* **2017**, *17*, 2920–2932. [[CrossRef](#)] [[PubMed](#)]

206. Feizi, A.; Zhang, Y.; Greenbaum, A.; Guziak, A.; Luong, M.; Chan, R.Y.L.; Berg, B.; Ozkan, H.; Luo, W.; Wu, M.; et al. Rapid, portable and cost-effective yeast cell viability and concentration analysis using lensfree on-chip microscopy and machine learning. *Lab Chip* **2016**, *16*, 4350–4358. [[CrossRef](#)]
207. Nissim, N.; Dudaie, M.; Barnea, I.; Shaked, N.T. Real-Time Stain-Free Classification of Cancer Cells and Blood Cells Using Interferometric Phase Microscopy and Machine Learning. *Cytom. Part A* **2021**, *99*, 511–523. [[CrossRef](#)]
208. Hirotsu, A.; Kikuchi, H.; Yamada, H.; Ozaki, Y.; Haneda, R.; Kawata, S.; Murakami, T.; Matsumoto, T.; Hiramatsu, Y.; Kamiya, K.; et al. Artificial intelligence-based classification of peripheral blood nucleated cells using label-free imaging flow cytometry. *Lab Chip* **2022**, *22*, 3464–3474. [[CrossRef](#)]
209. Wu, J.L.; Xu, Y.Q.; Xu, J.J.; Wei, X.M.; Chan, A.C.; Tang, A.H.; Lau, A.K.; Chung, B.M.; Cheung Shum, H.; Lam, E.Y.; et al. Ultrafast laser-scanning time-stretch imaging at visible wavelengths. *Light. Sci. Appl.* **2017**, *6*, e16196. [[CrossRef](#)]
210. Pirone, D.; Sirico, D.; Miccio, L.; Bianco, V.; Mugnano, M.; Ferraro, P.; Memmolo, P. Speeding up reconstruction of 3D tomograms in holographic flow cytometry via deep learning. *Lab Chip* **2022**, *22*, 793–804. [[CrossRef](#)]
211. Jiang, Y.; Lei, C.; Yasumoto, A.; Kobayashi, H.; Aisaka, Y.; Ito, T.; Guo, B.; Nitta, N.; Kutsuna, N.; Ozeki, Y.; et al. Label-free detection of aggregated platelets in blood by machine-learning-aided optofluidic time-stretch microscopy. *Lab Chip* **2017**, *17*, 2426–2434. [[CrossRef](#)]
212. Guo, B.; Lei, C.; Kobayashi, H.; Ito, T.; Yalikun, Y.; Jiang, Y.; Tanaka, Y.; Ozeki, Y.; Goda, K. High-throughput, label-free, single-cell, microalgal lipid screening by machine-learning-equipped optofluidic time-stretch quantitative phase microscopy. *Cytom. Part A* **2017**, *91*, 494–502. [[CrossRef](#)] [[PubMed](#)]
213. Li, Y.; Mahjoubfar, A.; Chen, C.L.; Niazi, K.R.; Pei, L.; Jalali, B. Deep Cytometry: Deep learning with Real-time Inference in Cell Sorting and Flow Cytometry. *Sci. Rep.* **2019**, *9*, 11088. [[CrossRef](#)]
214. Lee, K.C.; Wang, M.; Cheah, K.S.; Chan, G.C.; So, H.K.; Wong, K.K.; Tsia, K.K. Quantitative Phase Imaging Flow Cytometry for Ultra-Large-Scale Single-Cell Biophysical Phenotyping. *Cytom. Part A* **2019**, *95*, 510–520. [[CrossRef](#)] [[PubMed](#)]
215. Yip, G.G.K.; Lo, M.C.K.; Yan, W.; Lee, K.C.M.; Lai, Q.T.K.; Wong, K.K.Y.; Tsia, K.K. Multimodal FACED imaging for large-scale single-cell morphological profiling. *APL Photonics* **2021**, *6*, 070801. [[CrossRef](#)]
216. Wu, Y.; Zhou, Y.; Huang, C.J.; Huang, C.J.; Kobayashi, H.; Kobayashi, H.; Yan, S.; Ozeki, Y.; Wu, Y.; Sun, C.W.; et al. Intelligent frequency-shifted optofluidic time-stretch quantitative phase imaging. *Opt. Express* **2020**, *28*, 519–532. [[CrossRef](#)]
217. Joshi, K.; Javani, A.; Park, J.; Velasco, V.; Xu, B.; Razorenova, O.; Esfandyarpour, R. A Machine Learning-Assisted Nanoparticle-Printed Biochip for Real-Time Single Cancer Cell Analysis. *Adv. Biosyst.* **2020**, *4*, 2000160. [[CrossRef](#)]
218. Honrado, C.; McGrath, J.S.; Reale, R.; Bisegna, P.; Swami, N.S.; Caselli, F. A neural network approach for real-time particle/cell characterization in microfluidic impedance cytometry. *Anal. Bioanal. Chem.* **2020**, *412*, 3835–3845. [[CrossRef](#)]
219. Wang, N.; Liu, R.; Asmare, N.; Chu, C.H.; Civalekoglu, O.; Sarioglu, A.F. Closed-loop feedback control of microfluidic cell manipulation via deep-learning integrated sensor networks. *Lab Chip* **2021**, *21*, 1916–1928. [[CrossRef](#)]
220. Feng, Y.; Cheng, Z.; Chai, H.; He, W.; Huang, L.; Wang, W. Neural network-enhanced real-time impedance flow cytometry for single-cell intrinsic characterization. *Lab Chip* **2022**, *22*, 240–249. [[CrossRef](#)]
221. Caselli, F.; Reale, R.; Ninno, A.D.; Spencer, D.; Morgan, H.; Bisegna, P. Deciphering impedance cytometry signals with neural networks. *Lab Chip* **2022**, *22*, 1714–1722. [[CrossRef](#)]
222. Robinson, J.P. Flow cytometry: Past and future. *BioTechniques* **2022**, *72*, 159–169. [[CrossRef](#)] [[PubMed](#)]
223. Gu, Y.; Zhang, A.C.; Han, Y.; Li, J.; Chen, C.; Lo, Y.H. Machine Learning Based Real-Time Image-Guided Cell Sorting and Classification. *Cytometry. Part A J. Int. Soc. Anal. Cytol.* **2019**, *95*, 499–509. [[CrossRef](#)]
224. Sesen, M.; Whyte, G. Image-Based Single Cell Sorting Automation in Droplet Microfluidics. *Sci. Rep.* **2020**, *10*, 8736. [[CrossRef](#)] [[PubMed](#)]
225. Lee, K.; Kim, S.E.; Doh, J.; Kim, K.; Chung, W.K. User-friendly image-activated microfluidic cell sorting technique using an optimized, fast deep learning algorithm. *Lab Chip* **2021**, *21*, 1798–1810. [[CrossRef](#)]
226. Nitta, N.; Sugimura, T.; Isozaki, A.; Mikami, H.; Hiraki, K.; Sakuma, S.; Iino, T.; Arai, F.; Endo, T.; Fujiwaki, Y.; et al. Intelligent Image-Activated Cell Sorting. *Cell* **2018**, *175*, 266–276.e13. [[CrossRef](#)] [[PubMed](#)]
227. Zhang, Y.; Ouyang, M.; Ray, A.; Liu, T.; Kong, J.; Bai, B.; Kim, D.; Guziak, A.; Luo, Y.; Feizi, A.; et al. Computational cytometer based on magnetically modulated coherent imaging and deep learning. *Light. Sci. Appl.* **2019**, *8*, 91. [[CrossRef](#)] [[PubMed](#)]
228. Isozaki, A.; Mikami, H.; Tezuka, H.; Matsumura, H.; Huang, K.; Akamine, M.; Hiramatsu, K.; Iino, T.; Ito, T.; Karakawa, H.; et al. Intelligent image-activated cell sorting 2.0. *Lab Chip* **2020**, *20*, 2263–2273. [[CrossRef](#)]
229. McCallum, C.; Riordon, J.; Wang, Y.; Kong, T.; You, J.B.; Sanner, S.; Lagunov, A.; Hannam, T.G.; Jarvi, K.; Sinton, D. Deep learning-based selection of human sperm with high DNA integrity. *Commun. Biol.* **2019**, *2*, 1–10. [[CrossRef](#)] [[PubMed](#)]
230. Uslu, F.; Icoz, K.; Tasdemir, K.; Yilmaz, B. Automated quantification of immunomagnetic beads and leukemia cells from optical microscope images. *Biomed. Signal Process. Control* **2019**, *49*, 473–482. [[CrossRef](#)]
231. White, A.M.; Zhang, Y.; Shamul, J.G.; Xu, J.; Kwizera, E.A.; Jiang, B.; He, X. Deep Learning-Enabled Label-Free On-Chip Detection and Selective Extraction of Cell Aggregate-Laden Hydrogel Microcapsules. *Small* **2021**, *17*, 2100491. [[CrossRef](#)] [[PubMed](#)]
232. Christiansen, E.M.; Yang, S.J.; Ando, D.M.; Javaherian, A.; Skibinski, G.; Lipnick, S.; Mount, E.; O’Neil, A.; Shah, K.; Lee, A.K.; et al. In Silico Labeling: Predicting Fluorescent Labels in Unlabeled Images. *Cell* **2018**, *173*, 792–803.e19. [[CrossRef](#)]
233. Ounkomol, C.; Seshamani, S.; Maleckar, M.M.; Collman, F.; Johnson, G.R. Label-free prediction of three-dimensional fluorescence images from transmitted-light microscopy. *Nat. Methods* **2018**, *15*, 917–920. [[CrossRef](#)] [[PubMed](#)]

234. Kim, D.; Min, Y.; Oh, J.M.; Cho, Y.K. AI-powered transmitted light microscopy for functional analysis of live cells. *Sci. Rep.* **2019**, *9*, 18428. [[CrossRef](#)] [[PubMed](#)]
235. Bai, B.; Yang, X.; Li, Y.; Zhang, Y.; Pillar, N.; Ozcan, A. Deep learning-enabled virtual histological staining of biological samples. *Light. Sci. Appl.* **2023**, *12*, 57. [[CrossRef](#)]
236. Ugawa, M.; Kawamura, Y.; Toda, K.; Teranishi, K.; Morita, H.; Adachi, H.; Tamoto, R.; Nomaru, H.; Nakagawa, K.; Sugimoto, K.; et al. In silico-labeled ghost cytometry. *eLife* **2021**, *10*, e67660. [[CrossRef](#)]
237. Yang, D.; Zhou, Y.; Zhou, Y.; Han, J.; Ai, Y. Biophysical phenotyping of single cells using a differential multiconstriction microfluidic device with self-aligned 3D electrodes. *Biosens. Bioelectron.* **2019**, *133*, 16–23. [[CrossRef](#)]
238. Xiao, W.; Xin, L.; Cao, R.; Wu, X.; Tian, R.; Che, L.; Sun, L.; Ferraro, P.; Pan, F. Sensing morphogenesis of bone cells under microfluidic shear stress by holographic microscopy and automatic aberration compensation with deep learning. *Lab Chip* **2021**, *21*, 1385–1394. [[CrossRef](#)]
239. Soelistyo, C.J.; Vallardi, G.; Charras, G.; Lowe, A.R. Learning biophysical determinants of cell fate with deep neural networks. *Nat. Mach. Intell.* **2022**, *4*, 636–644. [[CrossRef](#)]
240. Combs, C.; Seith, D.D.; Bovyn, M.J.; Gross, S.P.; Xie, X.; Siwy, Z.S. Deep learning assisted mechanotyping of individual cells through repeated deformations and relaxations in undulating channels. *Biomicrofluidics* **2022**, *16*, 014104. [[CrossRef](#)]
241. Sarkar, S.; Kang, W.; Jiang, S.; Li, K.; Ray, S.; Luther, E.; Ivanov, A.R.; Fu, Y.; Konry, T. Machine learning-aided quantification of antibody-based cancer immunotherapy by natural killer cells in microfluidic droplets. *Lab Chip* **2020**, *20*, 2317–2327. [[CrossRef](#)] [[PubMed](#)]
242. Ao, Z.; Cai, H.; Wu, Z.; Hu, L.; Nunez, A.; Zhou, Z.; Liu, H.; Bondesson, M.; Lu, X.; Lu, X.; et al. Microfluidics guided by deep learning for cancer immunotherapy screening. *Proc. Natl. Acad. Sci.* **2022**, *119*, e2214569119. [[CrossRef](#)] [[PubMed](#)]
243. Honrado, C.; Salahi, A.; Adair, S.J.; Moore, J.H.; Bauer, T.W.; Swami, N.S. Automated biophysical classification of apoptotic pancreatic cancer cell subpopulations by using machine learning approaches with impedance cytometry. *Lab Chip* **2022**, *22*, 3708–3720. [[CrossRef](#)]
244. Whitfield, M.L.; Sherlock, G.; Saldanha, A.J.; Murray, J.I.; Ball, C.A.; Alexander, K.E.; Matese, J.C.; Perou, C.M.; Hurt, M.M.; Brown, P.O.; et al. Identification of Genes Periodically Expressed in the Human Cell Cycle and Their Expression in Tumors. *Mol. Biol. Cell* **2002**, *13*, 1977–2000. [[CrossRef](#)]
245. Song, H.; Wang, Y.; Rosano, J.M.; Prabhakarpandian, B.; Garson, C.; Pant, K.; Lai, E. A microfluidic impedance flow cytometer for identification of differentiation state of stem cells. *Lab Chip* **2013**, *13*, 2300–2310. [[CrossRef](#)] [[PubMed](#)]
246. Eulenberg, P.; Köhler, N.; Blasi, T.; Filby, A.; Carpenter, A.E.; Rees, P.; Theis, F.J.; Wolf, F.A. Reconstructing cell cycle and disease progression using deep learning. *Nat. Commun.* **2017**, *8*, 463. [[CrossRef](#)]
247. Rappez, L.; Rakhalin, A.; Rigopoulos, A.; Nikolenko, S.; Alexandrov, T. DeepCycle reconstructs a cyclic cell cycle trajectory from unsegmented cell images using convolutional neural networks. *Mol. Syst. Biol.* **2020**, *16*, e9474. [[CrossRef](#)]
248. He, Y.R.; He, S.; Kandel, M.E.; Lee, Y.J.; Hu, C.; Sobh, N.; Anastasio, M.A.; Popescu, G. Cell Cycle Stage Classification Using Phase Imaging with Computational Specificity. *ACS Photonics* **2022**, *9*, 1264–1273. [[CrossRef](#)]
249. Ghafari, M.; Clark, J.; Guo, H.B.; Yu, R.; Sun, Y.; Dang, W.; Qin, H. Complementary performances of convolutional and capsule neural networks on classifying microfluidic images of dividing yeast cells. *PLoS ONE* **2021**, *16*, e0246988. [[CrossRef](#)]
250. Aspert, T.; Hentsch, D.; Charvin, G. DetecDiv, a generalist deep-learning platform for automated cell division tracking and survival analysis. *eLife* **2022**, *11*, e79519. [[CrossRef](#)]
251. Kusumoto, D.; Seki, T.; Sawada, H.; Kunitomi, A.; Katsuki, T.; Kimura, M.; Ito, S.; Komuro, J.; Hashimoto, H.; Fukuda, K.; et al. Anti-senescent drug screening by deep learning-based morphology senescence scoring. *Nat. Commun.* **2021**, *12*, 257. [[CrossRef](#)] [[PubMed](#)]
252. Heckenbach, I.; Mkrtchyan, G.V.; Ezra, M.B.; Bakula, D.; Madsen, J.S.; Nielsen, M.H.; Oró, D.; Osborne, B.; Covarrubias, A.J.; Iddo, M.L.; et al. Nuclear morphology is a deep learning biomarker of cellular senescence. *Nat. Aging* **2022**, *2*, 742–755. [[CrossRef](#)]
253. Ronneberger, O.; Fischer, P.; Brox, T. U-Net: Convolutional Networks for Biomedical Image Segmentation. In Proceedings of the Medical Image Computing and Computer-Assisted Intervention—MICCAI 2015, Munich, Germany, 5–9 October 2015; Navab, N., Hornegger, J., Wells, W.M., Frangi, A.F., Eds.; Springer International Publishing: Cham, Switzerland, 2015; Lecture Notes in Computer Science; pp. 234–241. [[CrossRef](#)]
254. Valen, D.A.V.; Kudo, T.; Lane, K.M.; Macklin, D.N.; Quach, N.T.; DeFelice, M.M.; Maayan, I.; Tanouchi, Y.; Ashley, E.A.; Covert, M.W. Deep Learning Automates the Quantitative Analysis of Individual Cells in Live-Cell Imaging Experiments. *PLoS Comput. Biol.* **2016**, *12*, e1005177. [[CrossRef](#)]
255. Tsai, H.F.; Gajda, J.; Sloan, T.F.W.; Rares, A.; Shen, A.Q. Usiigaci: Instance-aware cell tracking in stain-free phase contrast microscopy enabled by machine learning. *SoftwareX* **2019**, *9*, 230–237. [[CrossRef](#)]
256. Bove, A.; Gradeci, D.; Fujita, Y.; Banerjee, S.; Charras, G.; Lowe, A.R. Local cellular neighborhood controls proliferation in cell competition. *Mol. Biol. Cell* **2017**, *28*, 3215–3228. [[CrossRef](#)] [[PubMed](#)]
257. Wen, C.; Miura, T.; Voleti, V.; Yamaguchi, K.; Tsutsumi, M.; Yamamoto, K.; Otomo, K.; Fujie, Y.; Teramoto, T.; Ishihara, T.; et al. 3DeeCellTracker, a deep learning-based pipeline for segmenting and tracking cells in 3D time lapse images. *eLife* **2021**, *10*, e59187. [[CrossRef](#)]
258. Wang, A.; Zhang, Q.; Han, Y.; Megason, S.; Hormoz, S.; Mosaliganti, K.R.; Lam, J.C.K.; Li, V.O.K. A novel deep learning-based 3D cell segmentation framework for future image-based disease detection. *Sci. Rep.* **2022**, *12*, 342. [[CrossRef](#)]

259. Padovani, F.; Mairhörmann, B.; Falter-Braun, P.; Lengefeld, J.; Schmoller, K.M. Segmentation, tracking and cell cycle analysis of live-cell imaging data with Cell-ACDC. *BMC Biol.* **2022**, *20*, 174. [[CrossRef](#)]
260. Ershov, D.; Phan, M.S.; Pylvänäinen, J.W.; Rigaud, S.U.; Le Blanc, L.; Charles-Orszag, A.; Conway, J.R.W.; Laine, R.F.; Roy, N.H.; Bonazzi, D.; et al. TrackMate 7: Integrating state-of-the-art segmentation algorithms into tracking pipelines. *Nat. Methods* **2022**, *19*, 829–832. [[CrossRef](#)]
261. Alnahhas, R.N.; Winkle, J.J.; Hirning, A.J.; Karamched, B.; Ott, W.; Josić, K.; Bennett, M.R. Spatiotemporal Dynamics of Synthetic Microbial Consortia in Microfluidic Devices. *ACS Synth. Biol.* **2019**, *8*, 2051–2058. [[CrossRef](#)]
262. Lugagne, J.B.; Lin, H.; Dunlop, M.J. DeLTA: Automated cell segmentation, tracking, and lineage reconstruction using deep learning. *PLoS Comput. Biol.* **2020**, *16*, e1007673. [[CrossRef](#)] [[PubMed](#)]
263. O’Connor, O.M.; Alnahhas, R.N.; Lugagne, J.B.; Dunlop, M.J. DeLTA 2.0: A deep learning pipeline for quantifying single-cell spatial and temporal dynamics. *PLoS Comput. Biol.* **2022**, *18*, e1009797. [[CrossRef](#)] [[PubMed](#)]
264. Koldaeva, A.; Tsai, H.F.; Shen, A.Q.; Pigolotti, S. Population genetics in microchannels. *Proc. Natl. Acad. Sci.* **2022**, *119*, e2120821119. [[CrossRef](#)]
265. Ulicna, K.; Vallardi, G.; Charras, G.; Lowe, A.R. Automated Deep Lineage Tree Analysis Using a Bayesian Single Cell Tracking Approach. *Front. Comput. Sci.* **2021**, *3*, 734559. [[CrossRef](#)]
266. Wang, M.; Ong, L.L.S.; Dauwels, J.; Asada, H.H. Multicell migration tracking within angiogenic networks by deep learning-based segmentation and augmented Bayesian filtering. *J. Med. Imaging* **2018**, *5*, 024005. [[CrossRef](#)]
267. Tsai, H.F.; IJsspeert, C.; Shen, A.Q. Voltage-gated ion channels mediate the electrotaxis of glioblastoma cells in a hybrid PMMA/PDMS microdevice. *APL Bioeng.* **2020**, *4*, 036102. [[CrossRef](#)]
268. Stallmann, D.; Göpfert, J.P.; Schmitz, J.; Grünberger, A.; Hammer, B. Towards an automatic analysis of CHO-K1 suspension growth in microfluidic single-cell cultivation. *Bioinformatics* **2021**, *37*, 3632–3639. [[CrossRef](#)] [[PubMed](#)]
269. Kok, R.N.U.; Hebert, L.; Huelsz-Prince, G.; Goos, Y.J.; Zheng, X.; Bozek, K.; Stephens, G.J.; Tans, S.J.; Zon, J.S.v. OrganoidTracker: Efficient cell tracking using machine learning and manual error correction. *PLoS ONE* **2020**, *15*, e0240802. [[CrossRef](#)]
270. Sugawara, K.; Çevrim, Ç.; Averof, M. Tracking cell lineages in 3D by incremental deep learning. *eLife* **2022**, *11*, e69380. [[CrossRef](#)]
271. Johnson, K.B.; Wei, W.Q.; Weeraratne, D.; Frisse, M.E.; Misulis, K.; Rhee, K.; Zhao, J.; Snowdon, J.L. Precision Medicine, AI, and the Future of Personalized Health Care. *Clin. Transl. Sci.* **2021**, *14*, 86–93. [[CrossRef](#)]
272. Guo, S.C.; Tao, S.C.; Dawn, H. Microfluidics-based on-a-chip systems for isolating and analysing extracellular vesicles. *J. Extracell. Vesicles* **2018**, *7*, 1508271. [[CrossRef](#)]
273. Ayuso, J.M.; Virumbrales-Muñoz, M.; Lang, J.M.; Beebe, D.J. A role for microfluidic systems in precision medicine. *Nat. Commun.* **2022**, *13*, 3086. [[CrossRef](#)]
274. Van Norman, G.A. Limitations of Animal Studies for Predicting Toxicity in Clinical Trials: Part 2: Potential Alternatives to the Use of Animals in Preclinical Trials. *JACC Basic Transl. Sci.* **2020**, *5*, 387–397. [[CrossRef](#)] [[PubMed](#)]
275. van Berlo, D.; van de Steeg, E.; Amirabadi, H.E.; Masereeuw, R. The potential of multi-organ-on-chip models for assessment of drug disposition as alternative to animal testing. *Curr. Opin. Toxicol.* **2021**, *27*, 8–17. [[CrossRef](#)]
276. Ma, S.; Murphy, T.W.; Lu, C. Microfluidics for genome-wide studies involving next generation sequencing. *Biomicrofluidics* **2017**, *11*, 021501. [[CrossRef](#)]
277. Zhou, W.m.; Yan, Y.y.; Guo, Q.r.; Ji, H.; Wang, H.; Xu, T.t.; Makabel, B.; Pilarsky, C.; He, G.; Yu, X.y.; et al. Microfluidics applications for high-throughput single cell sequencing. *J. Nanobiotechnol.* **2021**, *19*, 312. [[CrossRef](#)] [[PubMed](#)]
278. Lamanna, J.; Scott, E.Y.; Edwards, H.S.; Chamberlain, M.D.; Dryden, M.D.M.; Peng, J.; Mair, B.; Lee, A.; Chan, C.; Sklavounos, A.A.; et al. Digital microfluidic isolation of single cells for -Omics. *Nat. Commun.* **2020**, *11*, 5632. [[CrossRef](#)]
279. Heydari, A.A.; Sindi, S.S. Deep learning in spatial transcriptomics: Learning from the next next-generation sequencing. *Biophys. Rev.* **2023**, *4*, 011306. [[CrossRef](#)]
280. Ko, J.; Bhagwat, N.; Yee, S.S.; Ortiz, N.; Sahmoud, A.; Black, T.; Aiello, N.M.; McKenzie, L.; O’Hara, M.; Redlinger, C.; et al. Combining Machine Learning and Nanofluidic Technology To Diagnose Pancreatic Cancer Using Exosomes. *ACS Nano* **2017**, *11*, 11182–11193. [[CrossRef](#)]
281. Low, L.A.; Mummary, C.; Berridge, B.R.; Austin, C.P.; Tagle, D.A. Organs-on-chips: Into the next decade. *Nat. Rev. Drug Discov.* **2021**, *20*, 345–361. [[CrossRef](#)] [[PubMed](#)]
282. Wang, Y.; Wang, L.; Guo, Y.; Zhu, Y.; Qin, J. Engineering stem cell-derived 3D brain organoids in a perfusable organ-on-a-chip system. *RSC Adv.* **2018**, *8*, 1677–1685. [[CrossRef](#)] [[PubMed](#)]
283. Yi, H.G.; Jeong, Y.H.; Kim, Y.; Choi, Y.J.; Moon, H.E.; Park, S.H.; Kang, K.S.; Bae, M.; Jang, J.; Youn, H.; et al. A bioprinted human-glioblastoma-on-a-chip for the identification of patient-specific responses to chemoradiotherapy. *Nat. Biomed. Eng.* **2019**, *3*, 509–519. [[CrossRef](#)] [[PubMed](#)]
284. Carvalho, D.J.; Kip, A.M.; Romitti, M.; Nazzari, M.; Tegel, A.; Stich, M.; Krause, C.; Caiment, F.; Costagliola, S.; Moroni, L.; et al. Thyroid-on-a-Chip: An Organoid Platform for In Vitro Assessment of Endocrine Disruption. *Adv. Healthc. Mater.* **2022**, *2201555*. [[CrossRef](#)]
285. Zhang, F.; Qu, K.Y.; Zhou, B.; Luo, Y.; Zhu, Z.; Pan, D.J.; Cui, C.; Zhu, Y.; Chen, M.L.; Huang, N.P. Design and fabrication of an integrated heart-on-a-chip platform for construction of cardiac tissue from human iPSC-derived cardiomyocytes and in situ evaluation of physiological function. *Biosens. Bioelectron.* **2021**, *179*, 113080. [[CrossRef](#)]

286. Lee, K.K.; McCauley, H.A.; Broda, T.R.; Kofron, M.J.; Wells, J.M.; Hong, C.I. Human stomach-on-a-chip with luminal flow and peristaltic-like motility. *Lab Chip* **2018**, *18*, 3079–3085. [CrossRef] [PubMed]
287. Kasendra, M.; Tovaglieri, A.; Sontheimer-Phelps, A.; Jalili-Firoozinezhad, S.; Bein, A.; Chalkiadaki, A.; Scholl, W.; Zhang, C.; Rickner, H.; Richmond, C.A.; et al. Development of a primary human Small Intestine-on-a-Chip using biopsy-derived organoids. *Sci. Rep.* **2018**, *8*, 2871. [CrossRef] [PubMed]
288. Chen, M.B.; Whisler, J.A.; Fröse, J.; Yu, C.; Shin, Y.; Kamm, R.D. On-chip human microvasculature assay for visualization and quantification of tumor cell extravasation dynamics. *Nat. Protoc.* **2017**, *12*, 865–880. [CrossRef]
289. Dellaquila, A.; Thomée, E.K.; McMillan, A.H.; Lesher-Pérez, S.C. Chapter 4—Lung-on-a-chip platforms for modeling disease pathogenesis. In *Organ-on-a-Chip*; Hoeng, J., Bovard, D., Peitsch, M.C., Eds.; Academic Press: Cambridge, MA, USA, 2020; pp. 133–180.
290. Banaeian, A.A.; Theobald, J.; Paukštyte, J.; Wölfl, S.; Adiels, C.B.; Goksör, M. Design and fabrication of a scalable liver-lobule-on-a-chip microphysiological platform. *Biofabrication* **2017**, *9*, 015014. [CrossRef] [PubMed]
291. Ashammakhi, N.; Wesseling-Perry, K.; Hasan, A.; Elkhammas, E.; Zhang, Y.S. Kidney-on-a-chip: Untapped opportunities. *Kidney Int.* **2018**, *94*, 1073–1086. [CrossRef] [PubMed]
292. Silva, P.N.; J. Green, B.; M. Altamentova, S.; V. Rocheleau, J. A microfluidic device designed to induce media flow throughout pancreatic islets while limiting shear-induced damage. *Lab Chip* **2013**, *13*, 4374–4384. [CrossRef]
293. Sharma, K.; Dhar, N.; Thacker, V.V.; Simonet, T.M.; Signorino-Gelo, F.; Knott, G.W.; McKinney, J.D. Dynamic persistence of UPEC intracellular bacterial communities in a human bladder-chip model of urinary tract infection. *eLife* **2021**, *10*, e66481. [CrossRef]
294. Polini, A.; Moroni, L. The convergence of high-tech emerging technologies into the next stage of organ-on-a-chips. *Biomater. Biosyst.* **2021**, *1*, 100012. [CrossRef] [PubMed]
295. De Chiara, F.; Ferret-Mifiana, A.; Ramón-Azcón, J. The Synergy between Organ-on-a-Chip and Artificial Intelligence for the Study of NAFLD: From Basic Science to Clinical Research. *Biomedicines* **2021**, *9*, 248. [CrossRef] [PubMed]
296. Petreus, T.; Cadogan, E.; Hughes, G.; Smith, A.; Pilla Reddy, V.; Lau, A.; O'Connor, M.J.; Critchlow, S.; Ashford, M.; Oplustil O'Connor, L. Tumour-on-chip microfluidic platform for assessment of drug pharmacokinetics and treatment response. *Commun. Biol.* **2021**, *4*, 1–11. [CrossRef]
297. Li, J.; Chen, J.; Bai, H.; Wang, H.; Hao, S.; Ding, Y.; Peng, B.; Zhang, J.; Li, L.; Huang, W. An Overview of Organs-on-Chips Based on Deep Learning. *Research* **2022**, *2022*, 9869518. . [CrossRef] [PubMed]
298. Paek, K.; Kim, S.; Tak, S.; Kim, M.K.; Park, J.; Chung, S.; Park, T.H.; Kim, J.A. A high-throughput biomimetic bone-on-a-chip platform with artificial intelligence-assisted image analysis for osteoporosis drug testing. *Bioeng. Transl. Med.* **2023**, *8*, e10313. [CrossRef] [PubMed]
299. Oliver, C.R.; Altemus, M.A.; Westerhof, T.M.; Cherian, H.; Cheng, X.; Dziubinski, M.; Wu, Z.; Yates, J.; Morikawa, A.; Heth, J.; et al. A platform for artificial intelligence based identification of the extravasation potential of cancer cells into the brain metastatic niche. *Lab Chip* **2019**, *19*, 1162–1173. [CrossRef]
300. Oliver, C.R.; Westerhof, T.M.; Castro, M.G.; Merajver, S.D. Quantifying the Brain Metastatic Tumor Micro-Environment using an Organ-On-A Chip 3D Model, Machine Learning, and Confocal Tomography. *J. Vis. Exp. JoVE* **2020**, *162*, e61654. [CrossRef]
301. Chong, L.H.; Ching, T.; Farm, H.J.; Grenci, G.; Chiam, K.H.; Toh, Y.C. Integration of a microfluidic multicellular coculture array with machine learning analysis to predict adverse cutaneous drug reactions. *Lab Chip* **2022**, *22*, 1890–1904. [CrossRef]
302. Jena, B.P.; Gatti, D.L.; Arslanturk, S.; Pernal, S.; Taatjes, D.J. Human skeletal muscle cell atlas: Unraveling cellular secrets utilizing ‘muscle-on-a-chip’, differential expansion microscopy, mass spectrometry, nanothermometry and machine learning. *Micron* **2019**, *117*, 55–59. [CrossRef]
303. Shannon, M.J.; Mace, E.M. Natural Killer Cell Integrins and Their Functions in Tissue Residency. *Front. Immunol.* **2021**, *12*, 647358. [CrossRef] [PubMed]
304. Parlato, S.; De Ninno, A.; Molfetta, R.; Toschi, E.; Salerno, D.; Mencattini, A.; Romagnoli, G.; Fragale, A.; Roccazzello, L.; Buoncervello, M.; et al. 3D Microfluidic model for evaluating immunotherapy efficacy by tracking dendritic cell behaviour toward tumor cells. *Sci. Rep.* **2017**, *7*, 1093. [CrossRef] [PubMed]
305. Biselli, E.; Agliari, E.; Barra, A.; Bertani, F.R.; Gerardino, A.; De Ninno, A.; Mencattini, A.; Di Giuseppe, D.; Mattei, F.; Schiavoni, G.; et al. Organs on chip approach: A tool to evaluate cancer -immune cells interactions. *Sci. Rep.* **2017**, *7*, 12737. [CrossRef] [PubMed]
306. Nguyen, M.; De Ninno, A.; Mencattini, A.; Mermet-Meillon, F.; Fornabaio, G.; Evans, S.S.; Cossutta, M.; Khira, Y.; Han, W.; Sirven, P.; et al. Dissecting Effects of Anti-cancer Drugs and Cancer-Associated Fibroblasts by On-Chip Reconstitution of Immunocompetent Tumor Microenvironments. *Cell Rep.* **2018**, *25*, 3884–3893.e3. [CrossRef]
307. Comes, M.C.; Casti, P.; Mencattini, A.; Di Giuseppe, D.; Mermet-Meillon, F.; De Ninno, A.; Parrini, M.C.; Businaro, L.; Di Natale, C.; Martinelli, E. The influence of spatial and temporal resolutions on the analysis of cell-cell interaction: A systematic study for time-lapse microscopy applications. *Sci. Rep.* **2019**, *9*, 6789. [CrossRef] [PubMed]
308. Mathur, L.; Ballinger, M.; Utharala, R.; Merten, C.A. Microfluidics as an Enabling Technology for Personalized Cancer Therapy. *Small* **2020**, *16*, 1904321. [CrossRef] [PubMed]
309. Blasiak, A.; Khong, J.; Kee, T. CURATE.AI: Optimizing Personalized Medicine with Artificial Intelligence. *SLAS Technol.* **2020**, *25*, 95–105. [CrossRef] [PubMed]

310. Blasiak, A.; Truong, A.T.L.; Wang, P.; Hooi, L.; Chye, D.H.; Tan, S.B.; You, K.; Remus, A.; Allen, D.M.; Chai, L.Y.A.; et al. IDentif.AI-Omicron: Harnessing an AI-Derived and Disease-Agnostic Platform to Pinpoint Combinatorial Therapies for Clinically Actionable Anti-SARS-CoV-2 Intervention. *ACS Nano* **2022**, *16*, 15141–15154. [[CrossRef](#)] [[PubMed](#)]
311. Ahuja, K.; Rather, G.M.; Lin, Z.; Sui, J.; Xie, P.; Le, T.; Bertino, J.R.; Javanmard, M. Toward point-of-care assessment of patient response: A portable tool for rapidly assessing cancer drug efficacy using multifrequency impedance cytometry and supervised machine learning. *Microsyst. Nanoeng.* **2019**, *5*, 1–11. [[CrossRef](#)]
312. Mencattini, A.; Di Giuseppe, D.; Comes, M.C.; Casti, P.; Corsi, F.; Bertani, F.R.; Ghibelli, L.; Businaro, L.; Di Natale, C.; Parrini, M.C.; et al. Discovering the hidden messages within cell trajectories using a deep learning approach for in vitro evaluation of cancer drug treatments. *Sci. Rep.* **2020**, *10*, 7653. [[CrossRef](#)]
313. Owh, C.; Ho, D.; Loh, X.J.; Xue, K. Towards machine learning for hydrogel drug delivery systems. *Trends Biotechnol.* **2023**, *41*, 476–479. [[CrossRef](#)] [[PubMed](#)]

**Disclaimer/Publisher's Note:** The statements, opinions and data contained in all publications are solely those of the individual author(s) and contributor(s) and not of MDPI and/or the editor(s). MDPI and/or the editor(s) disclaim responsibility for any injury to people or property resulting from any ideas, methods, instructions or products referred to in the content.